INTERNATIONAL ATOMIC ENERGY AGENCY
UNITED NATIONS EDUCATIONAL, SCIENTIFIC AND CULTURAL ORGANIZATION

INTERNATIONAL CENTRE FOR THEORETICAL PHYSICS
34100 TRIESTE (ITALY) - P.O.B. 586 - MIRAMARE - STRADA COSTIERA 11 - TELEPHONES: 224281/2/3/4/5/6
CABLE: CENTRATOM - TELEX 460392-1

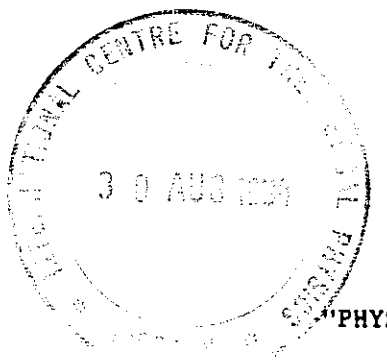

SMR/110/A - 12

WORKING PARTY

ON

"PHYSICS OF CONDENSED MATTER AT PLANETARY PRESSURES"

(20 August - 7 September 1984)

SOLID STATE CREEP
(Part I)

B.K. ATKINSON

Geology Dept., Imperial College,
London SW7 2BP, England

TRUE TRIAXIAL TEST

$\sigma_1 > \sigma_2 > \sigma_3$

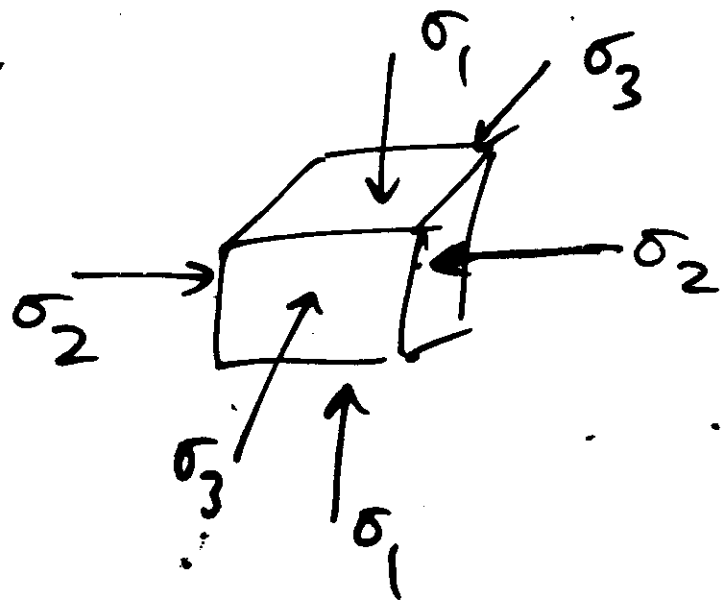

CONVENTIONAL TRIAXIAL TEST

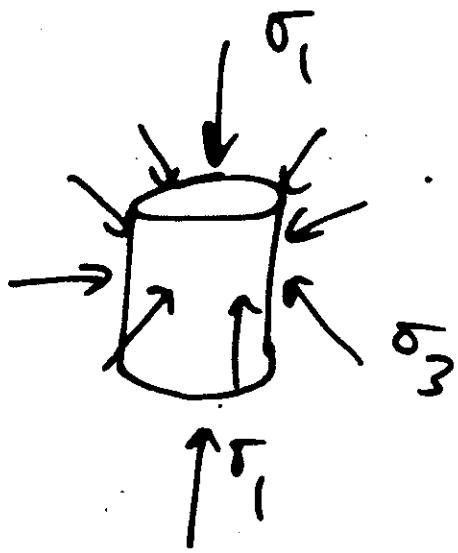

$\sigma_1 > \sigma_2 = \sigma_3$

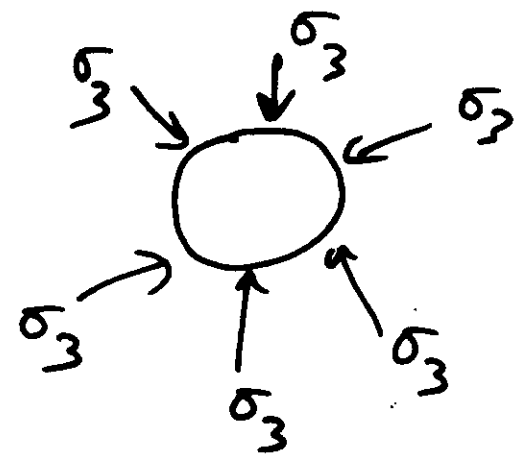

UNIAXIAL TEST

$\sigma_1 \geq \sigma_2 = \sigma_3 = 1b_0$

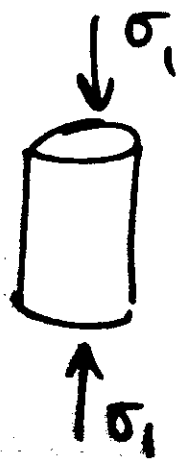

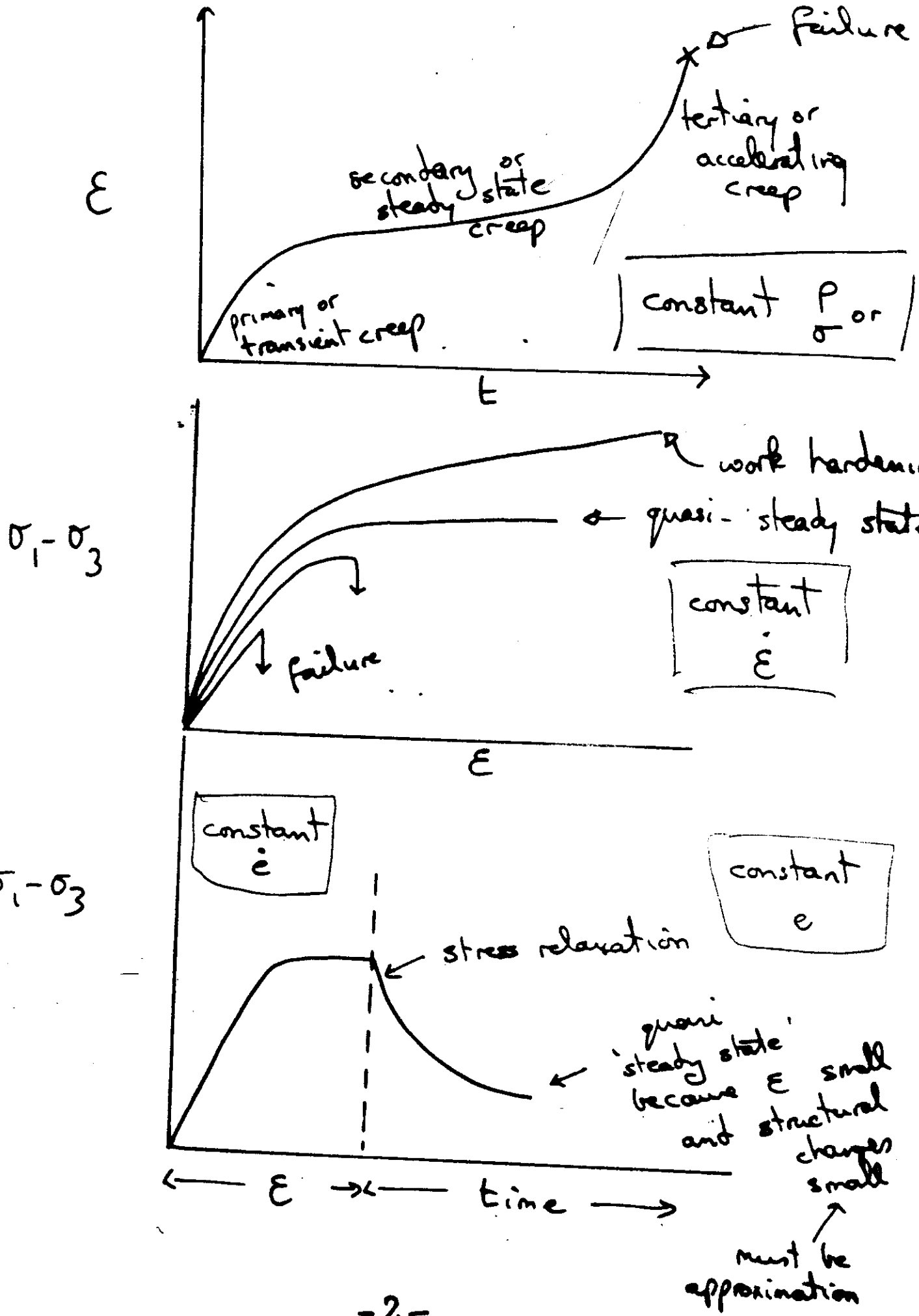
ε
failure
tertiary or accelerating creep
secondary or steady state creep
primary or transient creep
constant P or σ
t
σ1 - σ3
work hardening
quasi - steady state
constant ε̇
failure
ε
constant ε̇
constant ε
σ1 - σ3
stress relaxation
quasi 'steady state' because ε small and structural changes small
must be approximation
← ε →
time →

EVIDENCE FOR DEFORMATION MECHANISMS

① Laboratory studies → high pressure experiments

② Theoretical studies → deriving rate equations and matching predictions to observations

③ Field studies and microscopy plus texture studies X-ray, etc.

of rocks deformed in earth by natural tectonic (mountain building) processes.

MECHANISMS OF DEFORMATION

1. CATACLASIS : Involves NORMAL-PRESSURE dependent fracturing, brittle creep, frictional sliding, sub-critical cracking

2. DISLOCATION MECHANISMS :

Dislocation glide, dislocation creep (rate control is by dislocation climb — hence, may be diffusion-limited)

3. DIFFUSION AND GRAIN BOUNDARY SLIDING :

Diffusion path : grain boundary
volume
grain boundary films
fluid phase transport
vapour

Coble creep
Nabarro-Herring creep
Superplastic flow
(Recrystallization)
Pressure-solution → NOTEWORTHY : in that take place at temperatures below that even for dislocation creep.

CRUDE MECHANICAL ZONATION OF PLANETARY INTERIORS

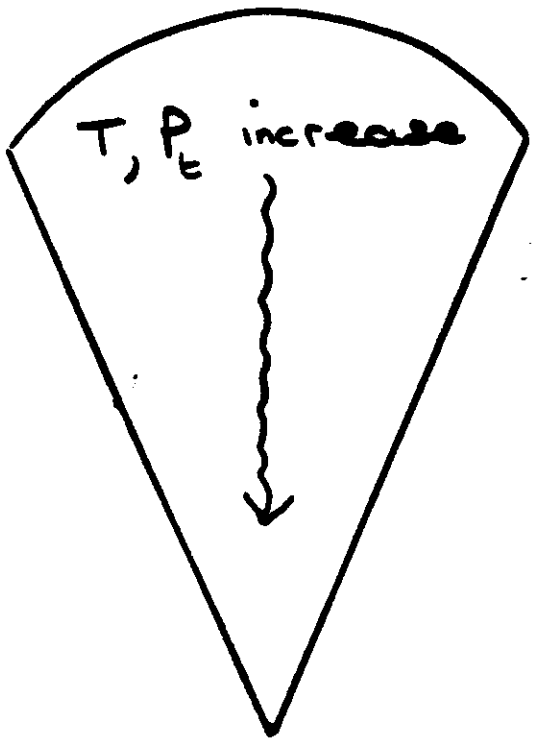

SURFACE

CATACLASTIC

BRITTLE CREEP

DISLOCATION FLOW

DIFFUSIONAL FLOW

increasing depth ↓

Inadequate! ESPECIALLY FOR EARTH because it ignores influence of:

1. Rock type

** 2. Pore fluids - especially water and its mechanical and chemical effects

← discussion of this will be a major theme of the lecture series

FACTORS THAT INFLUENCE THE MECHANICAL PROPERTIES OF ROCK

Environmental Variables

Temperature	T
Total Pressure	P_t
Effective Pressure	P_e
Pore fluid pressure	P_f

$$P_e = P_t - P_f$$

"law of effective stress"

Strain rate	$\dot{\varepsilon}$
Shear stress	τ
Volatile fugacity (partial pressure)	f_{O_2}, f_{H_2} etc

Material Variables

Grain size, shape, crystallographic orientation
Mineralogy, crystal structure (polymorphs)
Second phase particles
Stoichiometry (fugacity)
Internal structure - eg. dislocation density
Crack shape, size, distribution and arrangement.

α-β quartz

CATACLASIS

CLEAVAGE FRACTURE

No ENVIRONMENTAL EFFECTS INCLUDED

1. Upper limit to strength of solid is tensile stress to overcome inter atomic forces in perfect crystal

$$\sigma_{ideal} = \left(2E\Gamma_s/\pi b\right)^{\frac{1}{2}} \approx 0.1E$$

Γ_s = surface free energy; b = atomic size
E = Young's modulus

Flow is possible by continued granulation - stops when grains reach a size limited by ease of plasticity.

2. Pre-existing cracks prevent above situation being realized. They concentrate stress so that ideal stress is excelled at crack tip - even though applied stress $\ll \sigma_{ideal}$

$$\sigma_f = \left(2E\Gamma/\pi c_0\right)^{\frac{1}{2}}$$

$2c_0$ = crack length; Γ = fracture surface energy $> \Gamma_s$

EFFECT OF PRESSURE: Even in compression $\sigma_1 > \sigma_2 > \sigma_3$ get tensile stresses at crack tips.

CATACLASTIC FLOW

Model by 2 independent mechanisms (Atchby / Nerrull)

- granulation due to cleavage
- rolling and sliding (with no further fracture)

1. Granulation if

$$\sigma_s \geq \sigma_f + p \quad \text{if } p < \sigma_f$$

$$\sigma_s \geq 2(\sigma_f p)^{\frac{1}{2}} \quad \text{if } p \geq \sigma_f$$

σ_s = shear stress, p = hydrostatic pressure, σ_f = tensile fracture strength

2. Get rolling if

$$\sigma_s \geq p\left(\frac{1}{\sqrt{3}} + \sqrt{3}\mu_f\right)$$

(μ_f: coefficient of friction)

work done in dilation — work done against friction

Above = for cylinders rolling + sliding at contact points

Leads to volume expansion so (rolling) is much more pressure sensitive than granulation — thus suppressed at modest pressure and gives way to cleavage.

MODEL AS: (ASHBY/OVERALL)

$\dot{e} = \infty$ if either cleavage or rolling possible

$\dot{e} = 0$ if neither satisfied

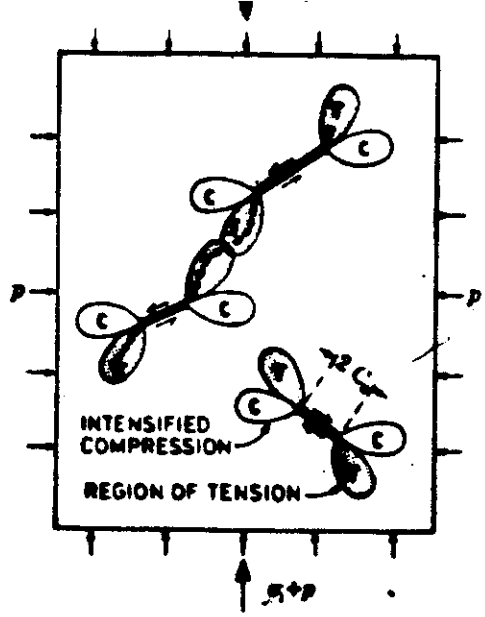

FIGURE 1. Cataclastic flow by cleavage. A deviatoric stress causes shearing displacements across the crack faces, generating tensile stresses in the regions marked T. If these reach a critical level, the cracks extend (broken lines) and ultimately link, even when the stress field is a compressive one.

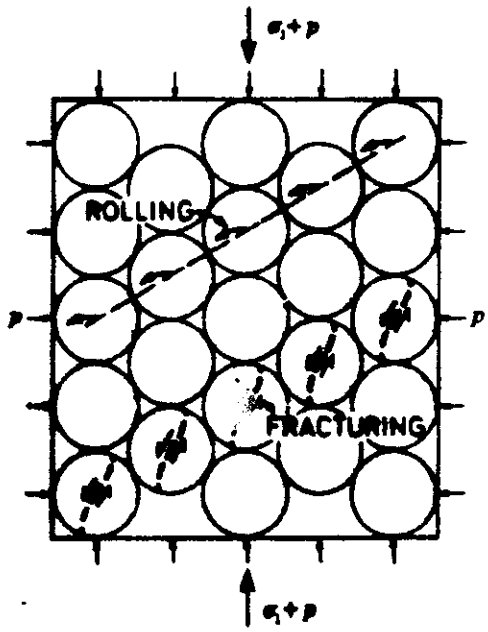

FIGURE 3. Granular or previously fractured materials can deform by the rolling and sliding of the granules or fragments over each other. Such flow is associated with a volume expansion, and because of this, it is more strongly influenced by pressure than is cleavage.

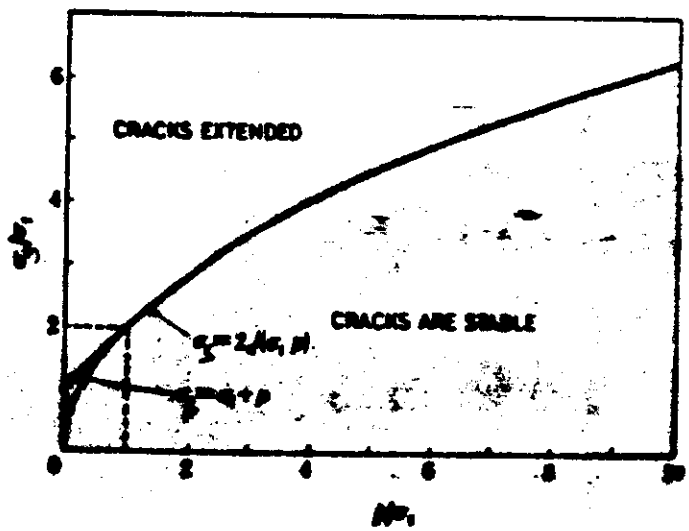

FIGURE 2. Griffith criterion, no friction. A plot of equations (9.4), showing how the [illegible] and shear cleavage (or cataclasis) increases with pressure, [illegible]

OTHER CLEAVAGE MECHANISMS

Subcritical crack growth

(i) - Stress corrosion
(ii) Diffusion
(iii) Plasticity (on micro scale)

Stress intensity factor

$$K = Y \sigma_a (\pi c)^{\frac{1}{2}}$$

2-D crack any mode (ie tensile, in-plane, anti-plane, shear)

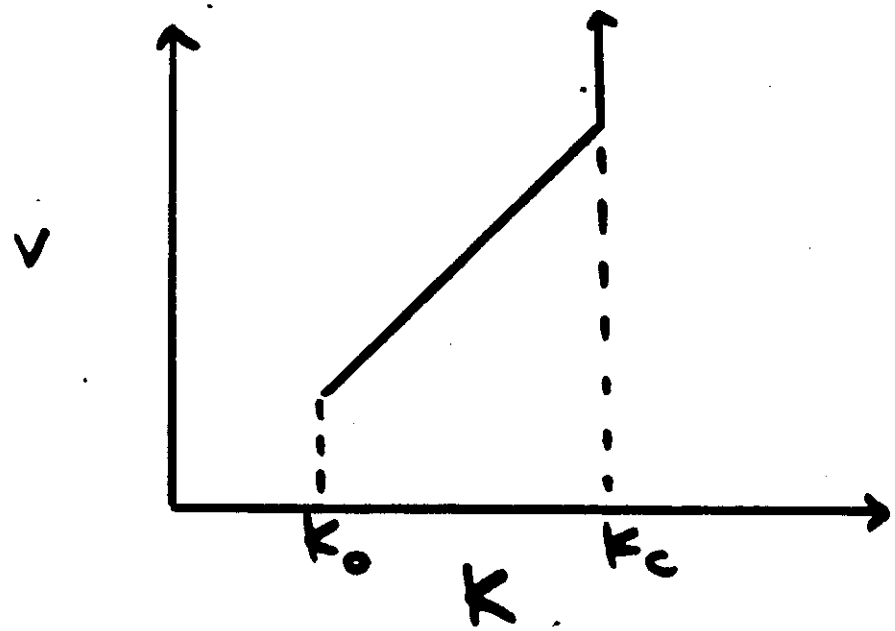

$$K_c = f(G_c) = f(\Gamma) \approx f(\Gamma_s)$$

Thus, when $\dot{\varepsilon}$ is slow (say $< 10^{-5} s^{-1}$) subcritical crack growth reduces σ_f for cleavage.

MUST INCLUDE ENVIRONMENTAL EFFECTS — SUBJECT OF SEPARATE LECTURE

LOW-TEMPERATURE PLASTICITY

DISLOCATION GLIDE

1. Plastic flow in crystalline solids by movement of dislocations on slip planes

2. If polycrystal is to deform homogeneously without fracture →
   5 INDEPENDENT SLIP SYSTEMS NEEDED
   Von Mises' criterion

   If non-homogeneous deformation allowed
   → 4 systems give compatible, but not uniform deformation

3. In silicates strong COVALENT bonds common and so strength of crystal fluctuates as dn moves
   Applied force or slope of energy/distance curve
   Peierls resistance or lattice resistance

4. Obstacles: impurities, precipitates, other dn's can also obstruct glide.
   Effect only visible if energy hill due to presence is greater than for intrinsic lattice resistance.

dn pile-ups at g.b.'s can lead to crack nucleation

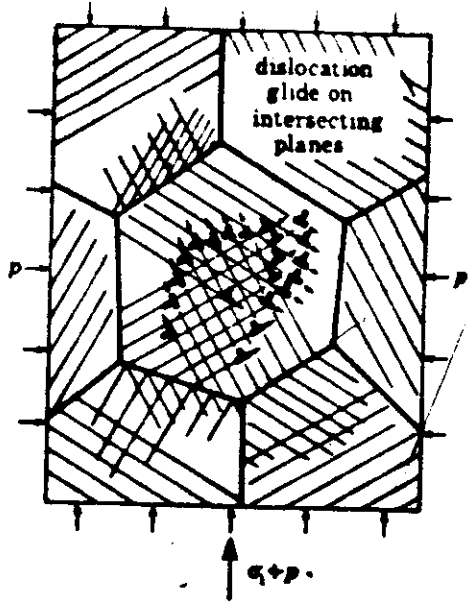

FIGURE 4. Low-temperature plasticity. The gliding motion of several sets of dislocations permits compatible deformation of the grains of a polycrystalline solid.

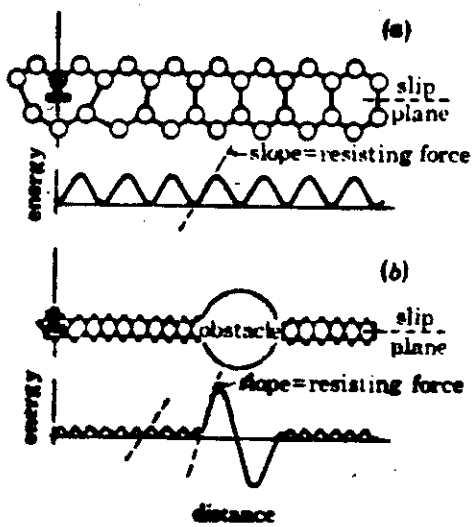

FIGURE 5. The yield strength reflects the force required to move a dislocation. In silicates such as olivine, the structure itself resists the motion, and the strength is said to be 'lattice resistance controlled' (*a*). Strong discrete obstacles – such as other dislocations – can sometimes determine the yield strength, which is then said to be 'obstacle-controlled' (*b*).

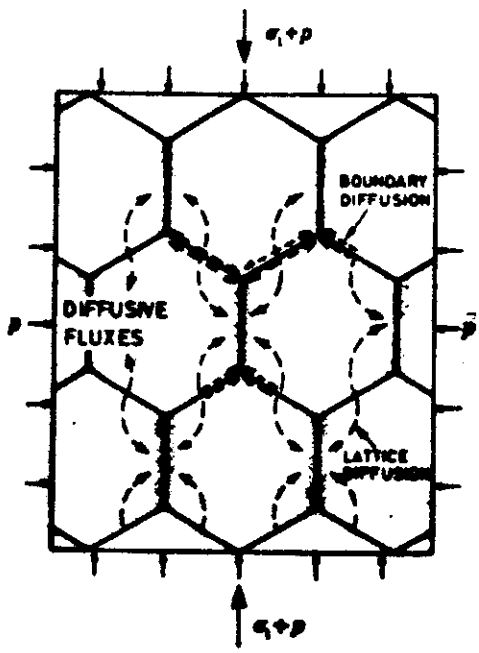

FIGURE 7. Diffusional flow. A deviatoric stress sets up differences in the chemical potential of [illegible] which then diffuse as shown by the broken lines, depositing in the [illegible]

DISLOCATION GLIDE

LATTICE RESISTANCE

$$\dot{e} = \dot{e}_p \left(\frac{\sigma_s}{\mu}\right)^2 \exp\left\{-\frac{\Delta F_p}{kT}\left[1-\left(\frac{\sigma_s}{\hat{\tau}_p}\right)^{3/4}\right]^{4/3}\right\}$$

$\dot{e}_p$ = pre-exponential constant
ΔF_p = act. energy for lattice resistance
$\hat{\tau}_p$ = flow stress at 0°K

Because ΔF_p small, strengthening due to lattice resistance drops as T raised until it is less than that of discrete obstacles

OBSTACLE RESISTANCE

$$\dot{e} = \dot{e}_o \exp\left\{(-\Delta F_o/kT)(1-\sigma_s/\hat{\tau}_o)\right\}$$

ΔF_o = act. energy for cutting/passing obstacles
$\hat{\tau}_o$ = flow stress at 0°K of obstacles acted above

Work hardening common - but flow stress saturates at strains $\gtrsim$ 1

DISLOCATION GLIDE

Effect of Pressure

lattice expansion due to pressure $\{dn$ is small compared to these terms

Account for by influence on ΔF_0, ΔF_p

$\hat{\tau}_0$, $\hat{\tau}_p$

ΔF scales as μb^3 } shear modulus and
$\hat{\tau}$ scales as μ } Burgers vector depend on pressure

e.g. b.c.c. metals $\Delta F \approx 0.07\,\mu b^3$
$\hat{\tau} \approx 0.01\,\mu$

μ increases more rapidly than b^3 decreases with pressure

Thus p raises ΔF and $\hat{\tau}$

$$d\left(\frac{\sigma_s}{\mu_0}\right) \Big/ d\left(\frac{p}{K_0}\right) = \left[\frac{K_0}{\mu_0}\frac{d\mu}{dp}\right]$$

K_0 = bulk modulus 300 K, 1 bar
μ_0 = shear modulus 300 K, 1 bar

As Temp. is raised (where $\hat{\tau}_0$, ΔF_0 increase with p)

$$\sigma_s = \hat{\tau}_0(p)\left\{1 - \left[kT/\Delta F_0(p)\right] \ln \frac{\dot{e}_0}{\dot{e}}\right\}$$

Thus:
At fried $(T, \dot{e})$ Pressure dependence of σ_s increases with increasing temperature

DIFFUSIONAL FLOW

Compressive stress raises chemical potential of ions on the grain boundaries.

If there is a difference in stress between boundaries and if atoms can be detached and re-attached freely then matter will flow through or round grains at a rate determined by diffusion.

If both lattice and grain boundary diffusion possible then (shear strain rate)

$$\dot{e} = 42\, D_{eff}\, \sigma_s\, \Omega / kT d^3$$

d = grain diameter Ω = atomic volume
D_{eff} = effective diffusion coefficient, d = grain size

For a one-component system

$$D_{eff} = D_V \left[1 + (\pi \delta / d)(D_B / D_V) \right]$$

D_V = lattice diffusion coefficient

δD_B = boundary diffusion path thickness × g.b. diffusion coefficient

If D_V fastest — Nabarro-Herring } creep
If δD_B fastest — Coble }

GRAIN BOUNDARY WIDTH

$\delta = 2b$ metals

But ionic/covalent solids have much larger disturbed region near free surface as absence of free electrons means that surface effects cannot be easily screened out

Where measurements have been made on ceramics

$\delta \simeq 10 \rightarrow 100\ b$

These seem more realistic for minerals

HOWEVER : Nature of grain boundary region in minerals in presence of interstitial pore fluids is one of major ignorance in rock deformation at present.

EFFECTIVE DIFFUSION IN MULTI-COMPONENT SYSTEMS

e.g. in 2- component system A_nB_m

$$D_V = \frac{D_V^A D_V^B}{(1-\chi_A) D_V^A + \chi_A D_V^B}$$

χ = atom- fraction of A in compound

The slower moving component determines the diffusion coefficient, and so limits the creep rate

Similar conclusion holds for >2 components.

e.g. In many oxides oxygen is the largest ion and the one which diffuses most slowly

Value of Ω also depends on nature of diffusing species

e.g. if O^{2-} limits mass transport in olivine $(Mg,Fe)_2SiO_4$

Arrival of one oxygen ion at grain boundary accompanied by $\frac{1}{4}$ silicon in and $\frac{1}{2}$ (Mg, Fe) in — in bulk

$\frac{1}{4}$ molecular volume of $(Mg,Fe)_2SiO_4$

$= \Omega$

SUPER PLASTIC FLOW

1. Continuity of material during diffusional flow only maintained if sliding displacements occur in the plane of the boundary

Diffusional flow can be regarded as diffusion-accomodated grain boundary sliding.

2. Implicit in derivation of diffusion creep equation is condition
   (a) grains must suffer same shape change as specimen itself
   (b) grains may not change neighbours

3. If constraints 2(a) and 2(b) relaxed, grains can slide past each other, change neighbours, and change shape by diffusion only where necessary to maintain continuity.

. This large strain variant of diffusion creep is known as SUPERPLASTIC CREEP

Rate equation has same form as that for diffusion creep, but is faster by a constant factor of ~ 5

INFLUENCE OF PRESSURE ON DIFFUSIONAL FLOW

Pressure slows diffusion because it increases the energy required for an atom to jump from one site to another, and because it may cause vacancy concentration to decrease.

Vacancy diffusion coefficient

$$D = \alpha a^2 n_v \omega$$

α = crystal structure factor (p independent)
a = lattice parameter (weakly p dependent)

Most pressure dependence is associated with

atom fraction of vacancies, n_v
and
frequency factor, ω

EFFECT OF PRESSURE ON VACANCY CONCENTRATION

Introducing a vacancy raises the volume of a solid by V_f

and work pV_f is done against external pressure, p.

Thus pressure increases vacancy formation energy and so vacancy concentration at thermal equilibrium decreases

$$\Delta G_f = \Delta G_f^\circ + pV_f$$

where superscript $^\circ$ = zero pressure, then

$$n_v = \exp\left\{-\left(\Delta G_f^\circ + pV_f\right)/kT\right\}$$

ΔG_f = energy of formation of vacancy.

Thus a linear increase in pressure → exponential decrease in vacancy concentration

In ionic substances removing ion exposes surrounding ionic shell to repulsive forces → large expansion up to $2\Omega^\circ$

Covalent - like hard shells → moderate expansion $\lesssim \Omega^\circ$

EFFECT OF PRESSURE ON VACANCY CONCENTRATION (2)

On simple arguments V_f should be $\simeq \Omega^\circ$

V_f ↓ volume expansion

Ω° ↓ effective atomic volume

COMPLICATION

Ionic compounds when doped with ions of different valency, adjust by creating vacancies of one species or interstitials of another to maintain CHARGE NEUTRALITY.
Pressure will not then change vacancy concentration

Oxides may not be stoichiometric, even when pure. Deviation from stoichiometry often achieved by creating vacancies on a sub-lattice eg oxygen.

The concentration of these vacancies is influenced by activity of volatiles in surrounding atmosphere
eg O_2, H_2, H_2O

so it is not net pressure, but partial pressure or fugacity of, for example, oxygen that determines rate of diffusion.

V_f may thus lie between 0 and Ω

EFFECT OF PRESSURE ON JUMP FREQUENCY

In diffusion an ion vibrating about one position jumps to a vacant position via an activated state.
During this jump its free energy of motion, ΔG_m increases the total free energy.

The frequency, ω, of such jumps is

$$\omega = \nu \exp\left(-\Delta G_m / kT\right)$$

ν = vibration frequency of atom in ground state.

In passing through an activated state an ion DISTORTS its surroundings.
If bonding is local (as in covalent) most of energy of motion goes into bond breaking and not elastic distortion and hence does not give as much volume expansion.

$$D = D^\circ\left(1 - 2p/3K^*\right)\exp\left(-pV^*/kT\right)$$

$$D^\circ = \alpha (a^*)^2 \nu \exp\left(-\left\{\Delta G_f + \Delta G_m\right\}/kT\right)$$

$= $ diffusion coefficient at zero pressure

and $V^* = V_f + V_m$ intrinsic diffusion

$V^* = V_m$ extrinsic diffusion

Measurements show $V^* \cong 0 \rightarrow 2\Omega$

DISLOCATION (POWER-LAW) CREEP

Between high-temperature regime of diffusional flow and low-temperature regime of dislocation glide plasticity

Creep occurs by: dn glide, dn climb and cell or polygon formation, gb sliding

Strain rate $\propto [\text{stress}]^n$

where $n = 3 \rightarrow 10$

Cell size is stress dependent. Cells have only slight ($\sim 2°$) angular misorientation.

Many sophisticated models for power-law creep - all give correct form of equation, but fail to accurately predict the constant n (or A; $\dot{e} = A\sigma^n$)

Can simply be regarded as a kind of diffusional flow where instead of grains, the sources and sinks for diffusional flow are the sub-grain, or cell, boundaries.

Add in the complication that

(i) because cells are smaller than grains - creep rate is fast

(ii) cell size itself depends on stress so creep is NOT Newtonian-viscous.

$$d_{cell}/_{atom\ size} \simeq \mu/\sigma_s$$

POWER-LAW CREEP

Creep Equation is

$$\dot{e} = A\left(D\mu b/kT\right)\left(\sigma_s/\mu\right)^n$$

A and n must be regarded as empirical quantities to be determined by experiment

Probably because there are several sorts of power-law creep.

USE WITH CAUTION: but Stocker/Ashby find EMPIRICAL relation

$$n \approx 3 + 0.3 \log A$$

OTHER PROBLEMS:

1. If stress $> 10^{-3}\mu$ power-law breaks down because dn glide makes a greater contribution to strain rate — get broad transition from power → exponential creep.

2. At high temperatures material may recrystallize as it creeps.
The waves of recrystallization wash out the cells and give rise to repeated surges of primary creep.

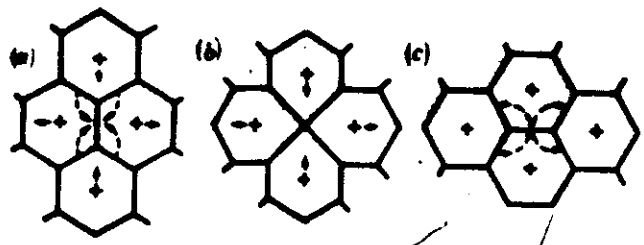

FIGURE 8. Diffusional flow when strains are large. If grains change their neighbours, the sample can undergo a large deformation while the grains alter their shape only slightly. At small strains (*a*) the diffusive paths, and the creep rate, are identical with those of figure 7, but at large strains (*b*) and (*c*)) the paths differ and the rate is higher. Superplasticity in metals can be explained in this way.

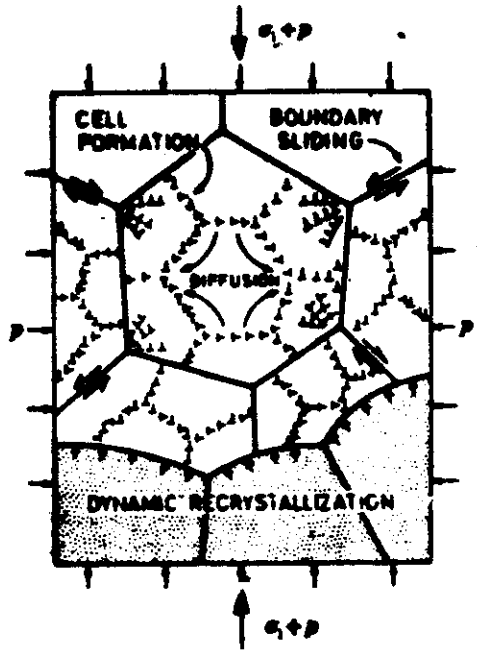

FIGURE 10. Power-law creep. The cells which form are the basis of the model described in the text, but the creep is complicated by grain-boundary sliding and by periodic recrystallization.

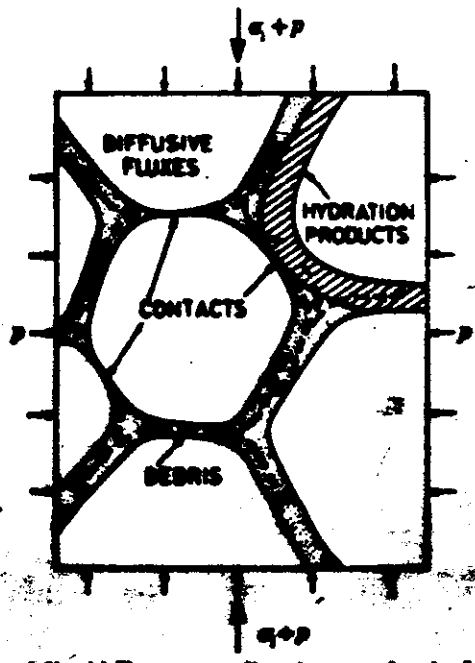

FIGURE 11. Fluid phase transport. A liquid film surrounding the granules in the Earth's crust, it might be water, in the mantle, a basaltic melt. The film provides a high-mobility path for the transport of ions of the solid, permitting creep, but its thickness at the critical points of contact is found to equilibrate

INFLUENCE OF PRESSURE ON POWER LAW CREEP

Activation volume - V^* shows its influence

Material	Structure	V^*/Ω° diffusion	V^*/Ω° creep
Pb	fcc	0.8	0.76
Na	bcc	0.4	0.41
Zn	hcp	0.55	0.65
AgBr	rock salt	1.9	1.9
Sn	tetragonal	0.3	0.31
P	tetragonal	0.5	0.44

Thus: effect of pressure is mainly through its influence on diffusion rates.

FLUID PHASE TRANSPORT

Ubiquitous pore water in crust
Partial melt in mantle

→ fast diffusion liquid path

Various attempts to model this process as a creep mechanism.

All produce essentially a Coble-creep type equation with appropriately faster diffusion rates.

All models have great difficulty with predicting the width of the high diffusivity path at critical contact points.

PROBLEM: Stress can only be transferred between grains if the liquid is squeezed out at the contact point, or reduced to essentially molecular thickness.

Thickness of layer and diffusion rates in it are open questions.

Physically – there may be a porous solid hydration product – essentially a thick g. boundary or porous debris, such as clay particles may accumulate at g.b.s to allow rapid ionic transport. TREAT AS SEPARATE

INFLUENCE OF TEXTURE / FABRIC

1. Creep by dislocation motion leads to preferred crystallographic orientation
2. Diffusion creep destroys preferred orientation

Both give grain SHAPE orientation.

Flow involving dislocation motion may be accelerated or decelerated by presence of a texture — depends on orientation of stresses.

If texture near perfect - material behaves like a single crystal.

DYNAMIC RECRYSTALLIZATION

Above ca. $0.6\,T_m$ recrystallization + creep

The new g.b.'s remove cells and tangles of dislocations.

They soften the material and allow a new cycle of primary creep.

Enhancement of creep rate depends on number of waves of recrystallization per unit creep strain.

In materials with few easy slip systems,

e.g. Ice, dynamic recrystallization has a much more important influence on creep.
It seems to recrystalize locally throughout creep and thus relieve interfacial stresses that might otherwise lead to cracking.

HARPER - DORN CREEP

6. Existence of chemical stress is not enough to ensure a larger than normal dn density. The effect of the frequency of the T cycling as well as the change in point defect concentration caused by dn motion must be considered.

7. eg. if T cycle period is very small, amplitude of dn climb motion will be small and if the dn cannot climb the typical distance between dns in a T cycle then the T cycling cannot affect the overall dn density.

At very long T cycles re-equilibration of dn structure occurs

There is an optimum range of T frequency for HD creep

At shorter or longer periods the temperature cycling should not affect the dn density.

8. Thus HD creep, on above arguments, cannot be an important creep mechanism in the mantle where T fluctuations must have an exceedingly long time period.

HARPER - DORN CREEP

1. Weertman / Blacic believe that HD creep is an artifact of low-amplitude thermal cycling.

2. Poirier et al. find HD creep in $KZnF_3$ which they regard as a perovskite analogue for $MgSiO_3$ in the lower mantle. If true might imply Newtonian viscosity in lower mantle.

3. **PROBLEM:** Dislocation density in HD creep is virtually independent of stress, yet would have expected it to range over 3 orders of magnitude

4. If a cyclic stress of amplitude σ_c is placed on specimen in addition to applied stress, then if $\sigma_c \gg \sigma$ the dn density is determined by σ_c and not σ.

5. Cyclic mechanical stress in experiments is likely to be small, but a cyclic thermal stress may be present and its magnitude could be appreciable. Even if temperature amplitude of $\pm 1K \rightarrow \pm 2K$, and instantaneous value of point defect concentration lags behind instantaneous equilibrium value, a cyclic chemical stress will act on dns.

For typical values

$$\sigma_{cc} \simeq Q_f \underbrace{\delta T}_{\text{ampl of } T \text{ cycle}} / T\Omega$$

(Q_f = formation energy of defect (lattice vacancy))

$\sigma_{cc} \simeq 3-6$ MPa

which is large compared to max. stress in most HD experiments

HARPER – DORN CREEP

1. At high temperatures and low stresses creep of some materials is
   (i) linearly related to stress
   (ii) activation energy close to lattice diffusion
   (iii) BUT up to 3 orders of magnitude faster than predicted by Nabarro–Herring creep.
   (iv) Apparently INDEPENDENT of grain size.

$$\frac{kT}{D G b}\,\dot{\gamma}_{HD} = A\left(\frac{\sigma_s}{G}\right)$$

2. Transition from HD to NH creep at a grain size d_c given by

$$d_c = b\,(B/A)^{1/2}$$

(B: numerical const. in NH creep equation)

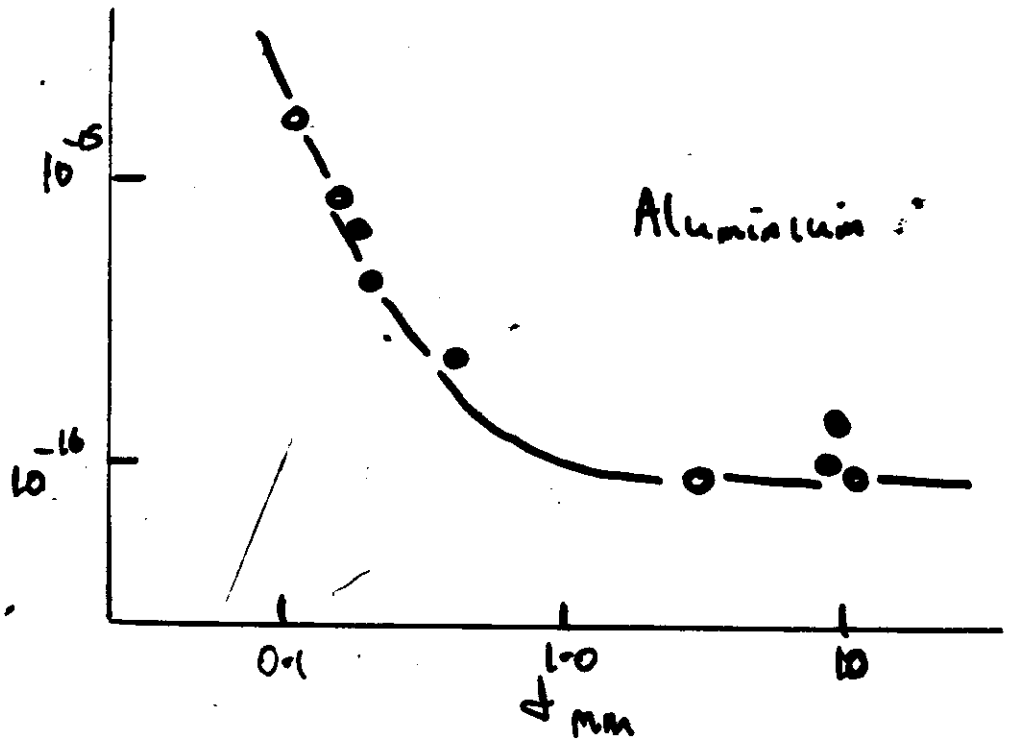

3. Explanations based on various dislocation theories proposed, but none widely accepted.

INTERPRETATION OF NATURAL ROCK TEXTURES

1. When using microscopic evidence of deformation mechanisms as guide to dominant mechanisms in nature – must be cautious.

2. Prograde metamorphism results in water release

   5-11% → 1·2% – bound water
   zeolite amphibolite

   ∴ high pore fluid pressures

3. Retrograde metamorphism, uplift + cooling leads to absorption of water.

   ∴ Fluid pressures will be lower than σ_3 porosity + permeability may be low until cracks form.

4. Thus any strain in retrograde metamorphism is likely to involve a different set of mechanisms to prograde metamorphism and this record will be imprinted on rocks returning to surface.

   Thus 'dry' def'nation textures might erroneously be thought to account for all strain the rock has sustained.

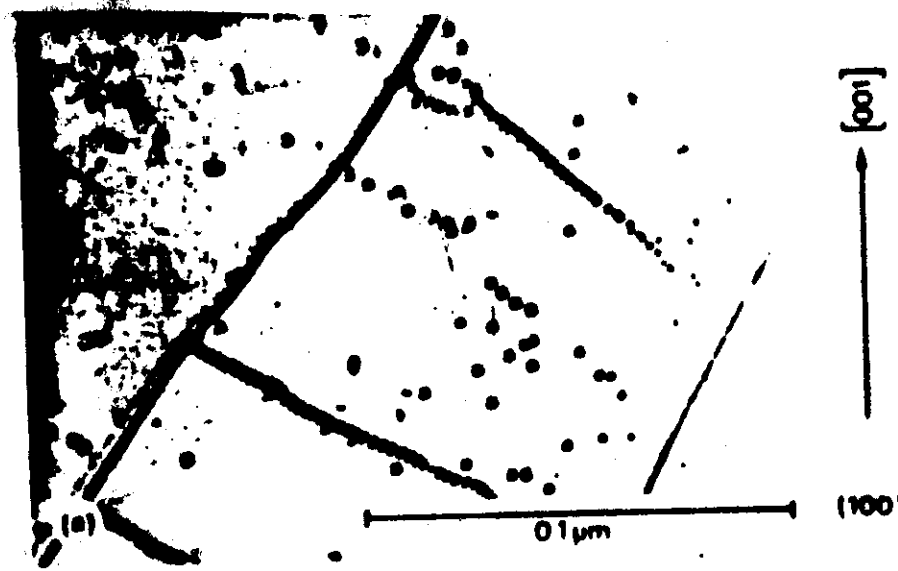

(a) Tilt subboundaries revealed by etch-pits on the (100) cleaved surface of halite single crystal. Creep deformation at $T = 700$ °C, $\sigma = 35$ g/mm^2, $\varepsilon = 24$ %.

(b) Subgrains revealed by Berg-Barrett topogram in a spinel single crystal deformed by creep at $T = 1450$ °C, $\sigma = 5$ kg/mm^2, $\varepsilon = 7$ %. Surface (100). (Photograph by R. Duclos)

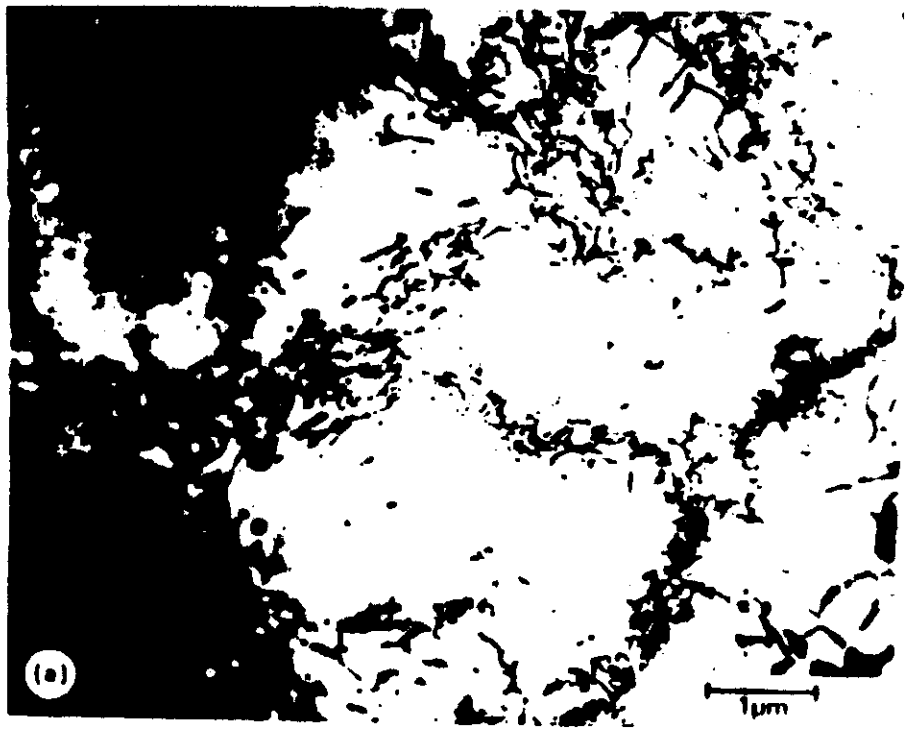

(a) Cellular dislocation structure in beryllium deformed at 175 °C (cold work) (TEM). The plane of the foil is (0001). (Photograph by J. Amelinckx)

(b) Dislocation wall enclosing a subgrain in an orthoclase crystal. Granite naturally deformed ($T = 500$ °C, $P = 2$ kbar) (TEM). (Photograph by M. Gandais, C. Gueth min. C. Willaime)

[illegible] FOR DEVELOPMENT OF DEFORMATION MAPS.

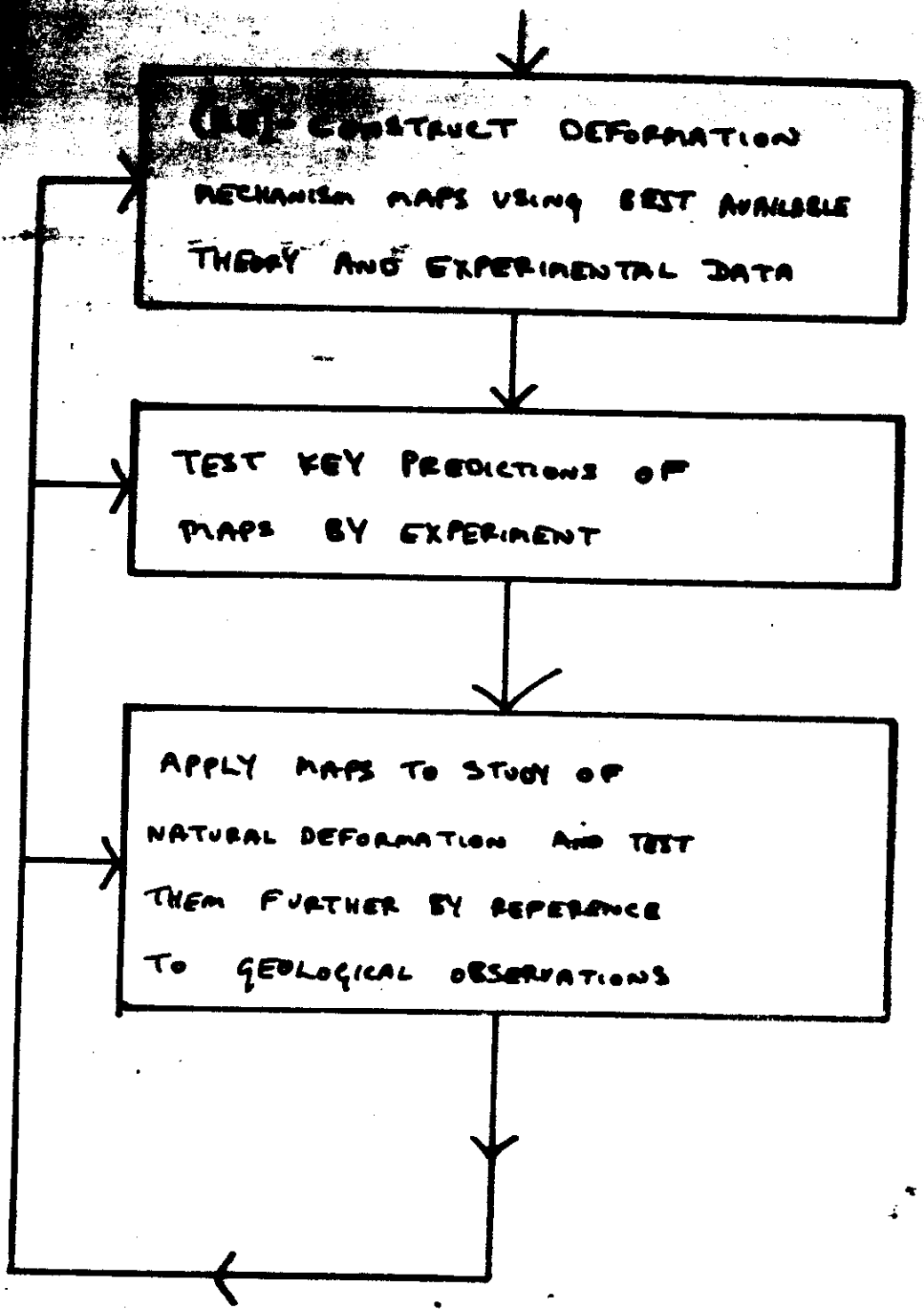

Stress exponent for DISLOCATION CREEP, n (PbS)

Ogden + Sherby (1973)

Binary compounds n falls into one of 2 groups depending upon relative sizes of compounds - constituent atomic species

Radius ratio < 2 $\quad n = 5$

Radius ratio > 2 $\quad n = 3$

From data of Pauling (1970) n for galena in high-temperature dislocation creep = 5.

This is compatible with High-temperature (700°C) creep experiments on single crystals of galena by Seltzer (1967), and Attwin (1978) on polycrystals.

But not with lower temperature (200° - 400°C) constant strain rate experiments by Attwin (1976). who found $n = .7$.

Resolve by considering 2 variants of dislocation creep.

→ low-temperature (in core diffusion controlled)

$$\dot{\varepsilon} \propto \sigma^{n+2} \propto \sigma^{7}$$

→ high-temperature (volume diffusion controlled)

$$\dot{\varepsilon} \propto \sigma^{n} \propto \sigma^{5}$$

LIMITATIONS OF MAPS

1. Consider only steady-state plastic flow. Cataclastic- and strain-dependent effects ignored, or modelled crudely.

2. Not all possible mechanisms of plastic flow considered:
   e.g. "Superplastic" flow
   Because of the lack of acceptable rate equations.

   N.B. incorporation of a new mechanism may radically alter the form of a deformation-mechanism map.

3. Calculation of strain rate contours is rather artificial. Ignores contribution to total strain rate of mechanisms in adjacent fields.
   Near field boundaries there are substantial regions of stress where 2 or more mechanisms make comparable contributions to the total strain rate.
   e.g. SLIDE . grain size : 4×10^{-4} m

   This has important microstructural implications.
   e.g. shape change of grains may be mainly by diffusion creep
   yet after deformation probably only dislocation creep leaves easily discernible evidence behind.

4. MAPS ARE ONLY AS GOOD AS THEIR DATA BASE

GEOLOGICAL APPLICATIONS OF DEFORMATION MECHANISM MAPS

From form of maps, if we know any 3 of variables stress, temperature, strain rate and grain size:

(1) we can identify the dominant mechanism
(2) we can estimate the value of the 4th variable.

GALENA

		Example: Mt. Isa, Australia	Rosebery, Tasmania
ASSUMPTIONS	Temperature:	200°C	300°C
	Grain size: (before metamorphism)	10 μm	10 μm
	Strain rate (folding)	$10^{-11} \rightarrow 10^{-14}$ s^{-1}	$10^{-11} \rightarrow 10^{-14}$ s^{-1}
INFERENCES	Dominant mechanism	COBLE CREEP	COBLE CREEP
	Steady state flow stresses	0·17 → 110 bars	$2 \cdot 8 \times 10^{-3} \rightarrow 2 \cdot 8$ bars
		$1 \cdot 7 \times 10^{4} \rightarrow 1 \cdot 1 \times 10^{7}$ Pa	$2 \cdot 8 \times 10^{2}$ Pa → $2 \cdot 8 \times 10^{6}$ Pa

MARK F. LINKER AND STEPHEN H. KIRBY

U.S. Geological Survey, 345 Middlefield Road, Menlo Park, California 94025

Samples cut from a hydrothermally grown synthetic quartz crystal with 370 ppm hydroxyl were tested at constant compressive load at atmospheric pressure over a range of temperature T = 400–800°C, axial stress σ = 800–2000 bar, and duration of load t = 37 min to 2 months. Two orientations of compression were chosen: O° (45° to [$2\bar{1}\bar{1}0$] and to [0001]) and $\perp m$ (perpendicular to ($01\bar{1}0$)). Plastic strains up to 10% shortening were achieved. Microcracking was minor or absent. We report the following contrasts in behavior in the two orientations of compression:

Orientation	O°	$\perp m$
Major slip system	($2\bar{1}\bar{1}0$) ⟨c⟩	Duplex ($10\bar{1}0$) ⟨a⟩
Creep curve shape		
Incubation stage	Accelerating creep rates	No significant incubation stage
Hardening stage	Decelerating creep rates	Hardening stage only
Tertiary stage	Failure only for T = 600–650°C	No tertiary stage
Relative creep rates	High	Low
Activation energies		
For creep, kcal mol^{-1}		
α-quartz field	52 ± 1	51 ± 3
β-quartz field	52 ± 2	38 ± 2
Stress exponent, n		
α-quartz field	3.0 ± 0.2	5.3 ± 0.5
β-quartz field		2.4 ± 0.3

TABLE 1. Experimental Flow Law Parameters, Synthetic Quartz Crystal X-507

Compression Orientation	$\log_{10}A$, bar^{-n}s^{-1}	Activation Energy for Creep, E_a*, kcal/mol: α-quartz field*	β-quartz field	α & β-quartz field	Stress Exponent, n: α-quartz field	β-quartz field
		E_a* determined at σ = 1400 bar				
O°	−8.9	52.3 ± 1.0			3.0 ± 0.2	
			21.7 ± 1.8			
				21.8 ± 0.4		
		E_a* determined at σ = 1000 bar				
O°		39.4 ± 0.5				
		E_a* determined at σ = 1400 bar				
$\perp m$	−8.5	50.9 ± 3.0			5.3 ± 0.5	
	−9.7		27.5 ± 1.8			2.4 ± 0.3
				34.6 ± 1.8		

*Strain rates picked at the maximum strain rate.

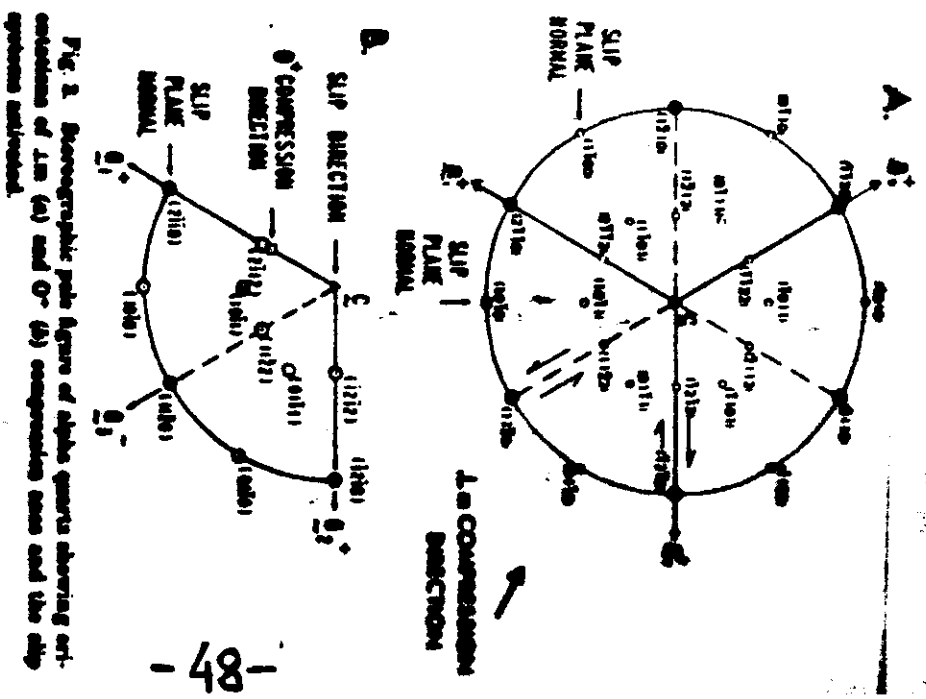

Fig. 2. Stereographic pole figure of alpha quartz showing orientations of ⊥m (a) and O° (b) compression axes and the slip systems activated.

TABLE 1. Slip Systems Identified in Quartz

α Quartz (32) $a = 4.91Å$, $c = 5.40Å$		β Quartz (622) $a = 5.02Å$, $c = 5.48Å$	
Direction	Plane	Direction	Plane
$\underline{a}$ $\langle 2\bar{1}\bar{1}0\rangle$	(0001) c $\{01\bar{1}1\}$ z $\{01\bar{1}\bar{1}\}$ r $\{01\bar{1}0\}$ m $\{0112\}$ v	$\underline{a}$ $\langle 2\bar{1}\bar{1}0\rangle$	(0001) c $\{1\bar{1}00\}$ m $\{01\bar{1}1\}$ z $\{01\bar{1}1\}$ r $\{01\bar{1}2\}$ v $\{01\bar{1}3\}$ w
$\underline{c}$ [0001]	$\{1\bar{1}00\}$ m $\{2\bar{1}\bar{1}0\}$ a	$\underline{c}$ [0001]	$\{1\bar{1}00\}$ m $\{2\bar{1}\bar{1}0\}$ a
$\langle \underline{c}+\underline{a}\rangle$ $\langle 2\bar{1}\bar{1}3\rangle$	$\{01\bar{1}0\}$ m $\{\bar{1}011\}$ z $\{\bar{2}112\}$ f	$\langle \underline{c}+\underline{a}\rangle$ $\langle 2\bar{1}\bar{1}3\rangle$	$\{01\bar{1}0\}$ m $\{\bar{1}011\}$ z $\{\bar{2}112\}$ f ?$\{11\bar{2}1\}$ g
		$\langle \underline{c}+2\underline{a}\rangle$ $\langle \bar{2}111\rangle$?	$10\bar{1}3$ u $11\bar{2}3$

Sources: Carter et al. [1964]; Christie et al. [1964a]: Christie and Green [1964]; Mieta and Ashbee [1967, 1969a]; Heard and Carter [1968]; Morrison-Smith [1974]; Morrison-Smith et al. [1976]; Twiss [1976]. Italicized letters with directions are the crystal axes and those with planes are the Dana symbols for the crystallographic forms [Frondel, 1962, p. 40]; these are commonly used instead of the slip planes in discussions of the slip systems.

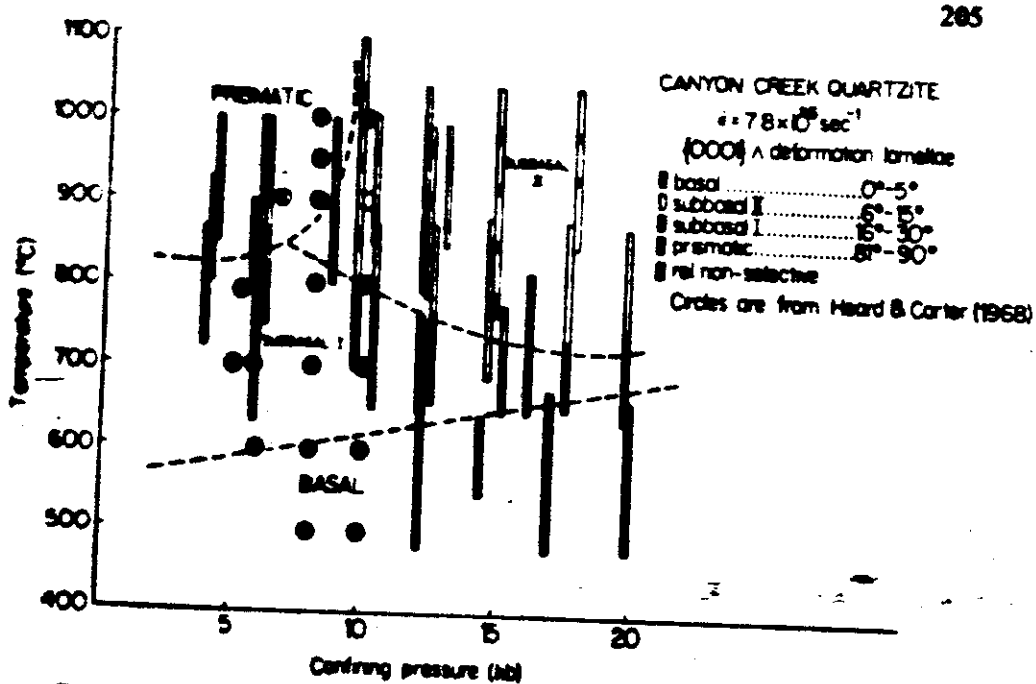

Fig. 5.28. Orientation of deformation lamellae (angle with (0001)) according to temperature and confining pressure for an experimentally deformed quartzite. (Reproduced by permission of The American Journal of Science, from Avé Lallemant and Carter, *Amer. J. Sci.*, 270, 218, Fig. 7 (1971))

Tilt dislocation wall in an enstatite grain of a peridotite nodule from kimberlites, equilibrated between 1200°C and 1400°C (TEM). Note stacking fault ribbons with fringed contrast (Photograph by Y. Gueguen)

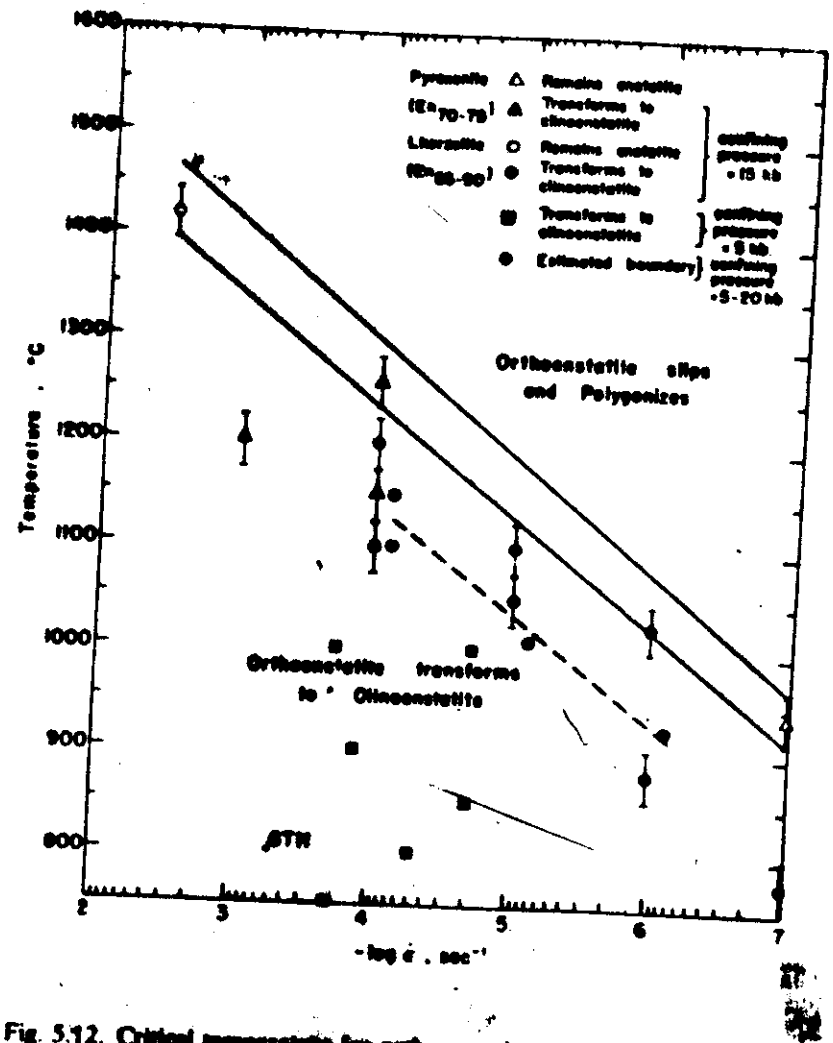

Fig. 5.12. Critical temperature for orthoenstatite to clinoenstatite inversion as a function of strain rate. GTH represents the experimental point of Griggs et al. (1960). (Reproduced with permission from Raleigh et al., *Jour. Geophys. Res.*, 76, 4011 (1971), copyright by American Geophysical Union)

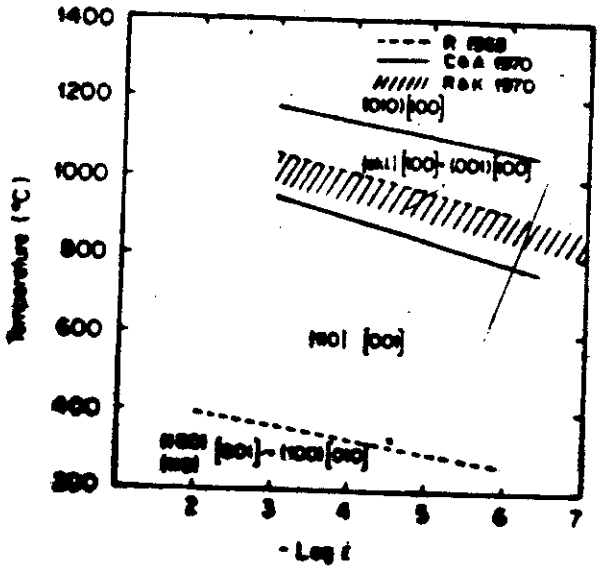

Fig. 5.3. Glide systems of olivine as a function of temperature and deformation rate

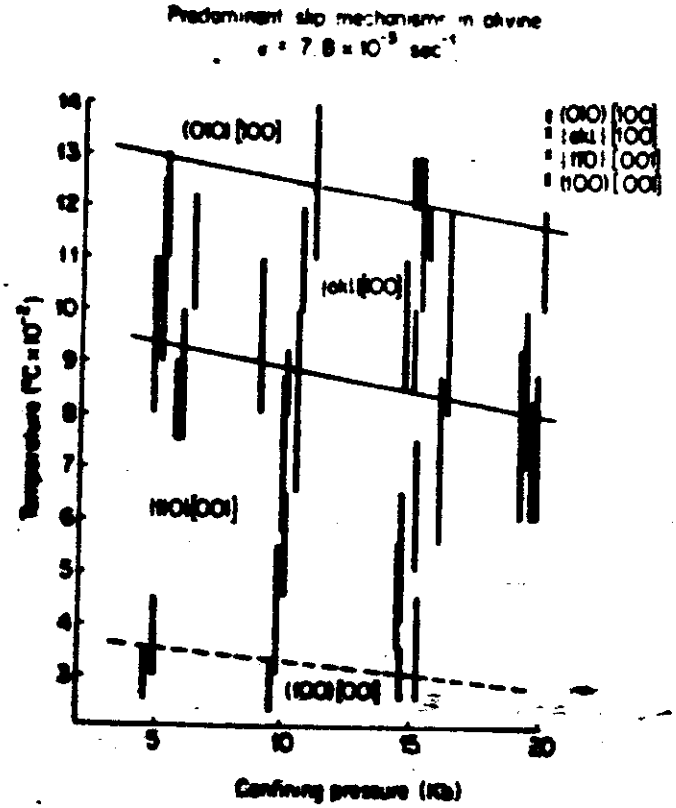

Fig. 5.4. Glide systems of olivine as a function of temperature and confining pressure (Carter and Ave'Lallemant, 1970). Vertical bars show results from single specimens in a given temperature range. (Reproduced by permission of The Geological Society of America)

TABLE 1. MATERIAL PROPERTIES FOR OLIVINE

material property	symbol	value	units	remarks
molecular volume per oxygen ion at 1 atm.†	Ω^*	1.53×10^{-29}	m^3	This value used for diffusional flow, equation (5.1)
oxygen ion volume at 1 atm.	Ω_i^*	1.15×10^{-29}	m^3	This value used for activation volumes, equation (5.9).
Burgers vector at 1 atm.	b^*	6.0×10^{-10}	m	An average of several values – § 4
melting point at 1 atm.	T_m	2140	K	
shear modulus at 300 K and 1 atm.	μ^*	8.13×10^{10}	Pa	See §§ 2.2 and 2.3 for references
T-dependence of shear modulus	$(T_m/\mu^*)(d\mu/dT)$	0.35	—	
P-dependence of shear modulus	$d\mu/dP$	1.8	—	
bulk modulus at 300 K and 1 atm.	K^*	1.27×10^{11}	Pa	See §§ 2.2 and 2.3 for references
T-dependence of bulk modulus	$(T_m/K^*)(dK/dT)$	0.28	—	
P-dependence of bulk modulus	dK/dP	5.1	—	
pre-exponential, lattice diffusion	D_{0v}	0.1	m^2/s	The data are discussed in § 5 and plotted in figure 9
activation energy, lattice diffusion	Q_v	522	kJ/mol	
activation volume/oxygen ion volume	V_v^*/Ω_i	0–1	—	
pre-exponential, boundary diffusion	δD_{0b}	1×10^{-10}	m^3/s	There are no data for olivine.
activation energy, boundary diffusion	Q_b	350	kJ/mol	These are obtained by scaling: $\delta D_{0b} = 10^{-4} D_{0v}$ and $Q_b = \frac{2}{3} Q_v$
activation volume/oxygen ion volume	V_b^*/Ω_i	0–1	—	
first creep exponent	n_1	3	—	See § 6.4 for the rate equation used for power-law creep. The values refer to creep in shear (equation (6.4))
second creep exponent	n_2	5	—	
first creep constant	A_1	0.65	—	
second creep constant	A_2	5.6×10^5	—	Q_{0v} and V_{0v}^* are the same as those for lattice diffusion
activation energy for creep	Q_{0v}	522	—	
activation volume/oxygen ion volume	V_{0v}^*/Ω_i	0–1		
flow stress at 0 K, (lattice resistance)/modulus	τ_p/μ	2.3×10^{-2}	—	This determines the flow stress at 0 K and throughout the plasticity field – see also § 4
pre-exponential for lattice resistance	$\dot{\gamma}_p$	10^{11}	s^{-1}	
activation energy for lattice resistance	$\Delta F_p/\mu b^3$	0.05	—	
flow stress at 0 K, (obstacle control)/modulus	τ_0/μ	8×10^{-4}	—	This determines the plateau in the flow stress separating plasticity from power-law creep – see also § 4
pre-exponential, obstacle control	$\dot{\gamma}_0$	10^6	s^{-1}	
activation energy for obstacle control	$\Delta F_0/\mu b^3$	0.5	—	
cleavage stress in tension modulus	σ_c/μ	5×10^{-2}	—	See § 3 and table 4

† 1 atm ≈ 10^5 Pa.

$\dot{\gamma} = \frac{[illegible]}{kT}\left[A_1\left(\frac{[illegible]}{\mu}\right)^{[illegible]} + A_2\left(\frac{[illegible]}{\mu}\right)^{[illegible]}\right]\exp\left(-\frac{[illegible]}{kT}\right)$

Note transition from n = 3 to n = 5

No convincing model for this so use empirical equation above.

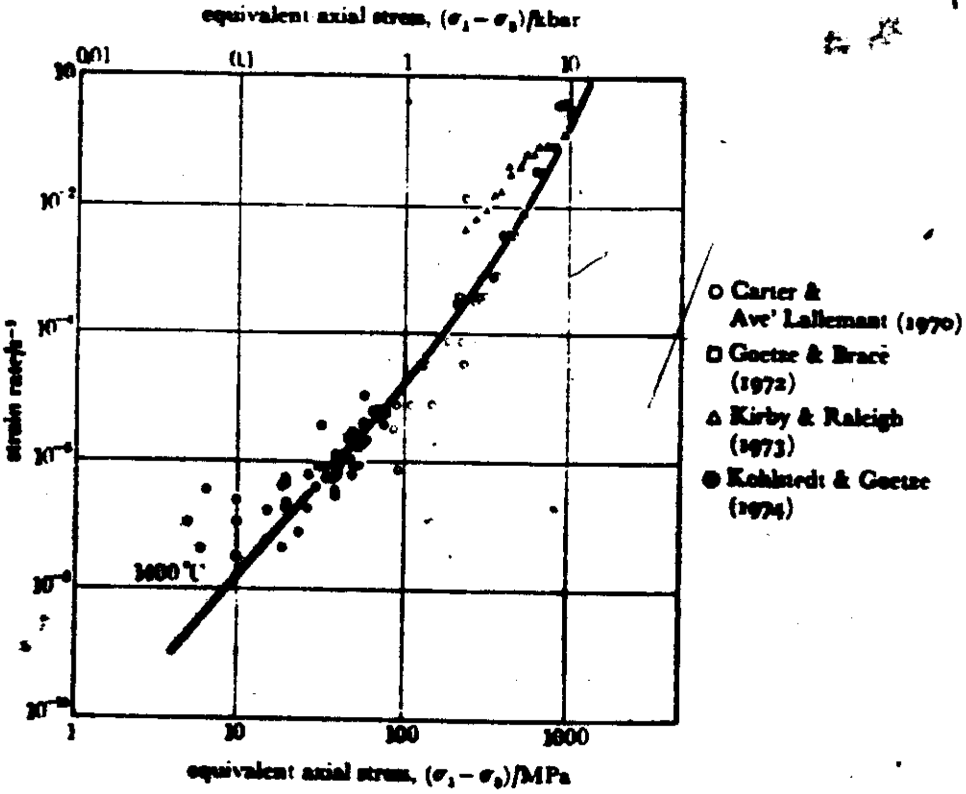

FIGURE 12. The creep of dry olivine. The data, normalized to a single temperature (1400 °C) by using an activation energy of 522 kJ/mol, are replotted from the work of Kohlstedt & Goetze (1974).

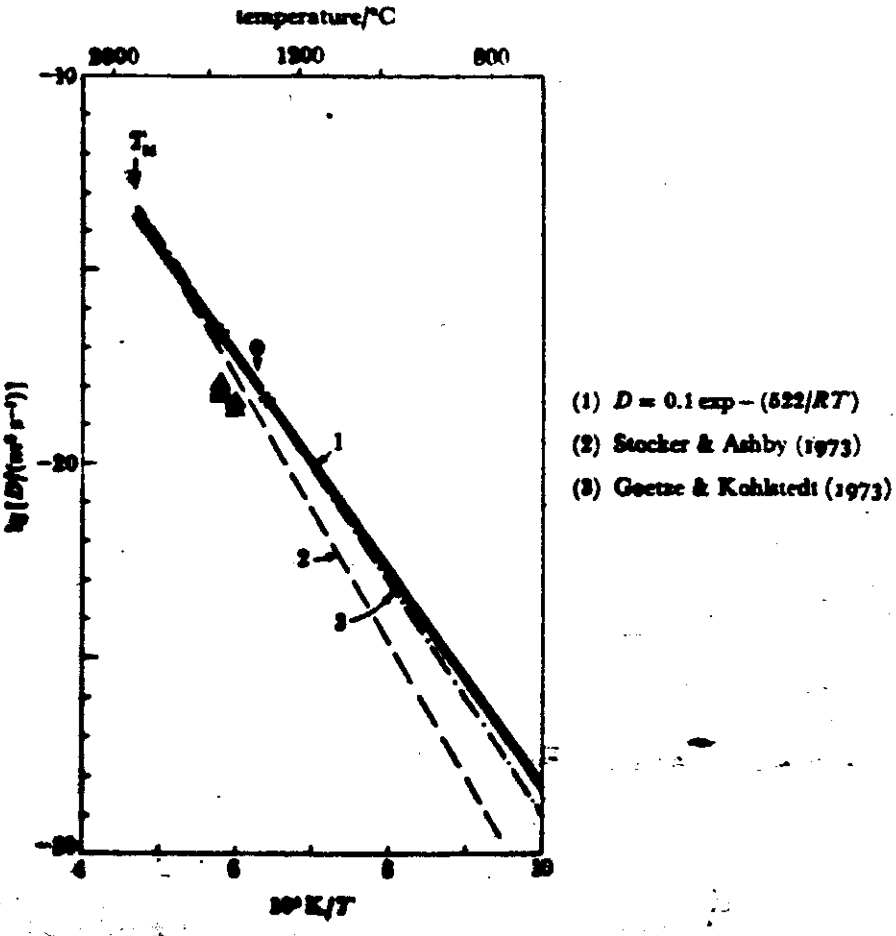

FIGURE 9. Diffusion [illegible] in olivine. The full line is a plot of the diffusion equation (equation (8.10)) used in §8 to [illegible] of diffusional flow. Data: ◆, Goetze & Kohlstedt (1973); ○, Borchardt & Schmalzried (1972); △, [illegible] ([illegible])

Fracture excluded for simplicity.

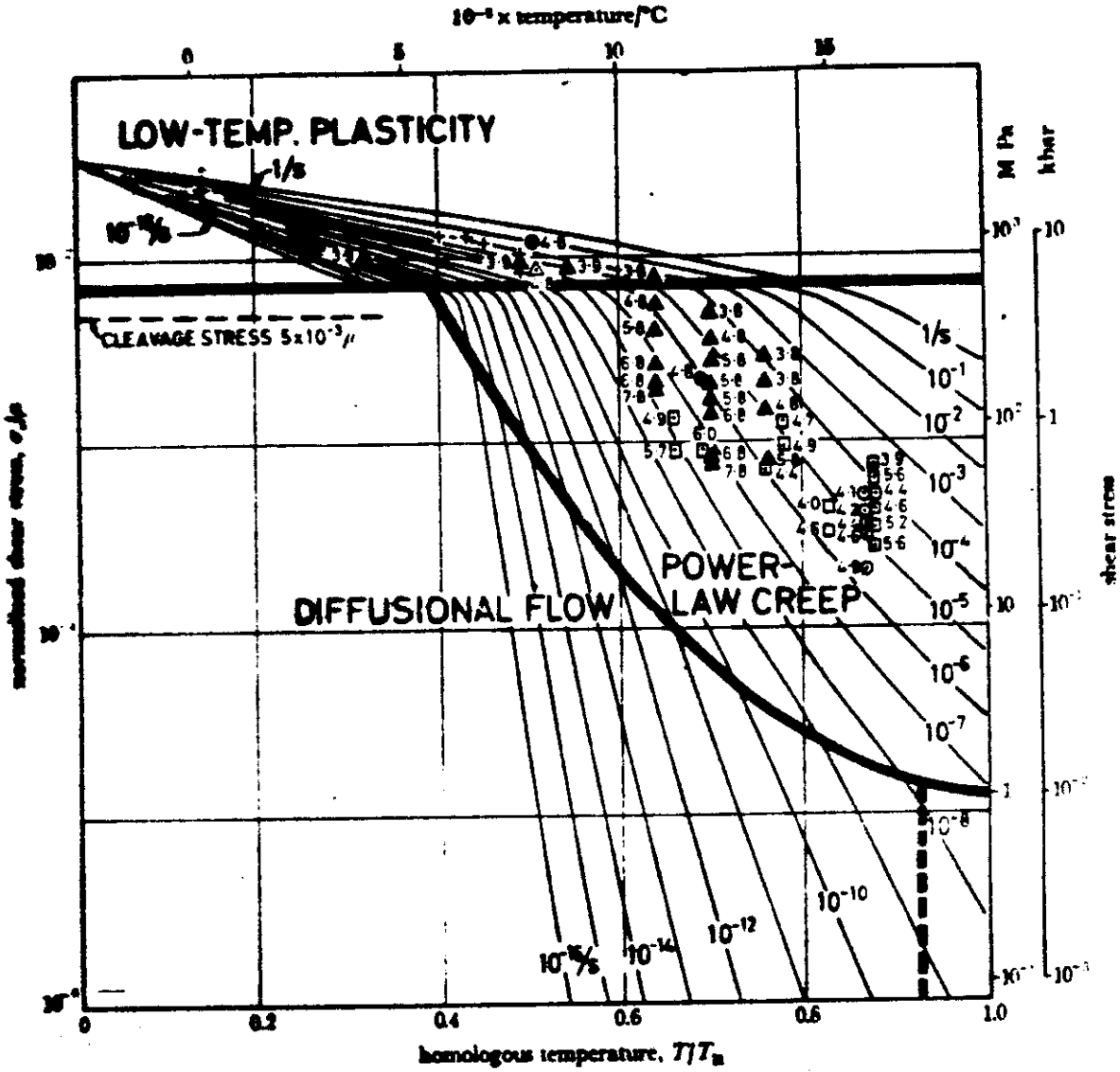

FIGURE 14. A map for olivine with a grain size of 0.1 mm; zero pressure. The symbols identify experimental points, and are labelled with the negative of the logarithm to the base 10 of the observed shear strain-rate. Cleavage was suppressed to show the plasticity field; if a realistic value for σ_c were used, the diagram would be truncated at the level marked 'cleavage stress $5\times10^{-3}\mu$'. Data: +, Evans (1976) hardness data; ▲, Carter & Ave' Lallemant (1970) (peridotite, 15 kbar); ●, Durham *et al.* (1976); ▲, Phakey *et al.* (1972) (single crystals, hard direction); ○, Kohlstedt & Goetze (1974); □, Durham & Goetze (1976).

P = 81 kb

Compared to
(1) cleavage stress raised
(2) plasticity stress raised
(3) strain rates slower

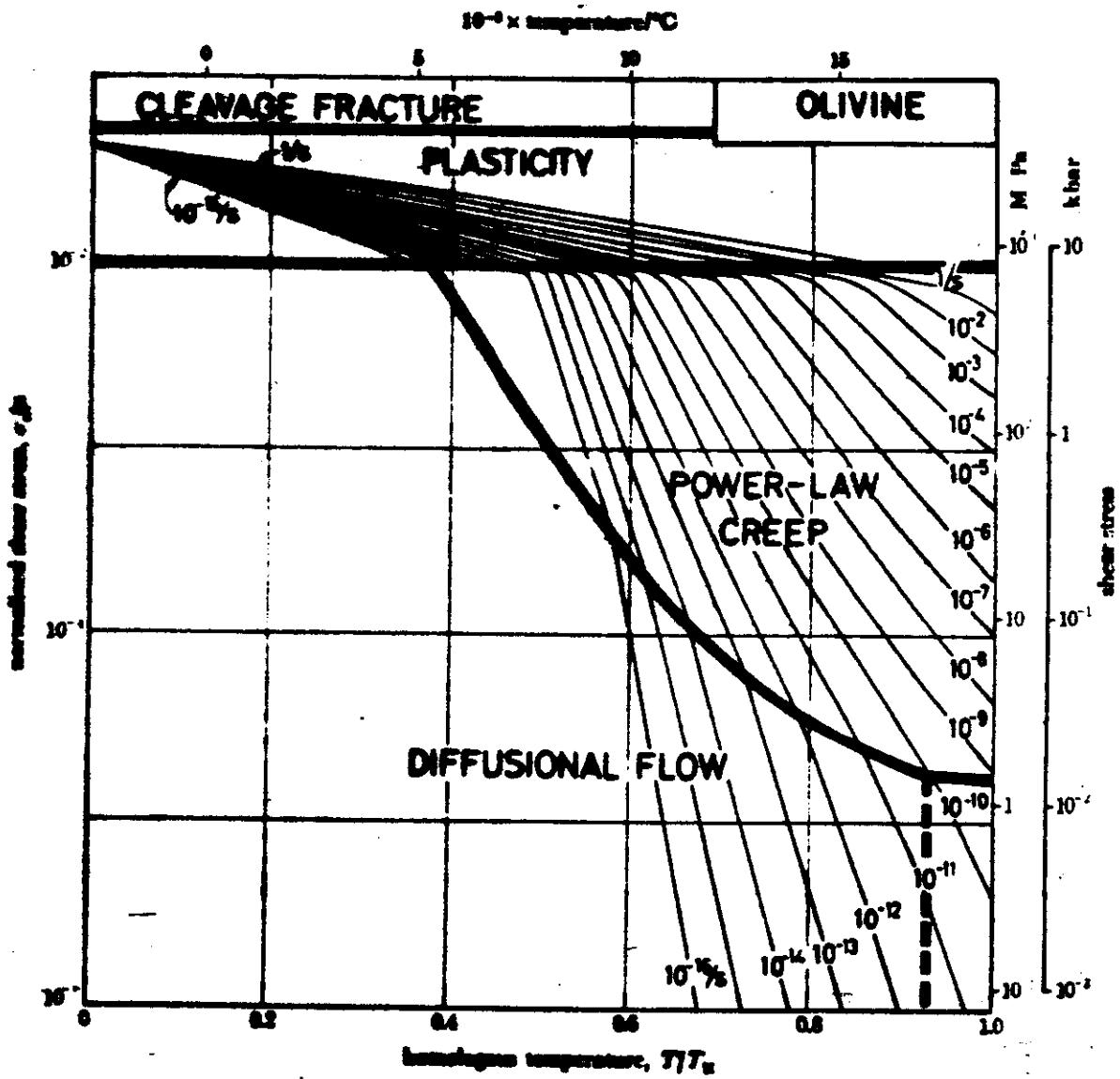

FIGURE 18. A map for olivine, based on the same data as figure 16, but with a pressure of 0.1 P_n (81 kbar) applied. The cleavage stress has been raised by a factor of about 10 to $8 \times 10^{-1}\,\mu$; the stress required for plasticity has increased by a factor of about 1.5 and the creep rates have decreased by a factor of about 10^4.

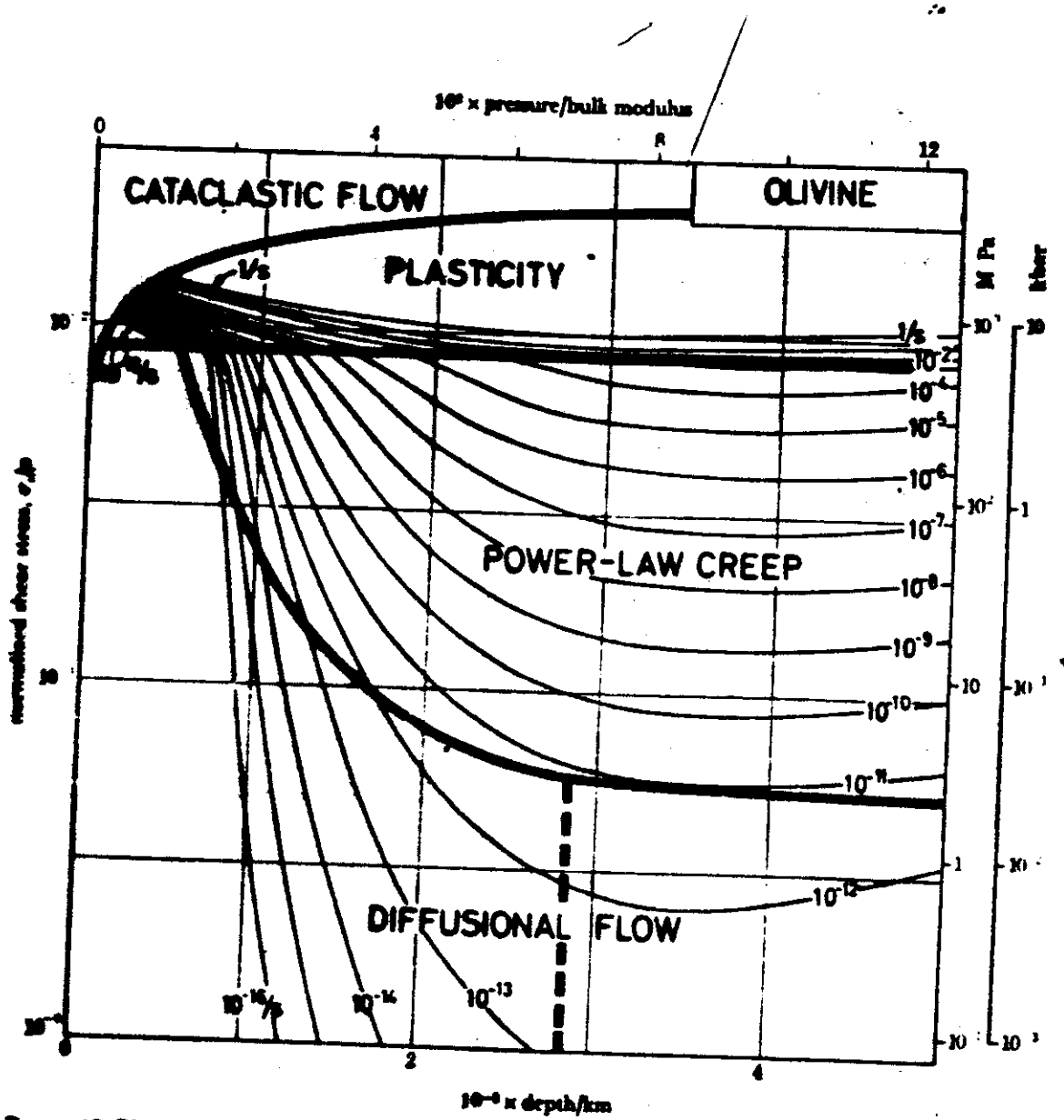

FIGURE 17. Olivine under upper-mantle conditions with $V^* = 0$; cleavage stress $= 5 \times 10^{-3}\mu$. In this figure, depth (below the Earth's surface) has replaced temperature as the abscissa; temperature and pressure are both related directly to it. The figure shows that, to a depth of about 20 km, cataclastic flow is the dominant mechanism. Below this, plasticity and creep replace fracturing as the dominant mechanisms.

① To depth of ca 30 km cataclastic flow a dominant mechanism

$V^* = 0$

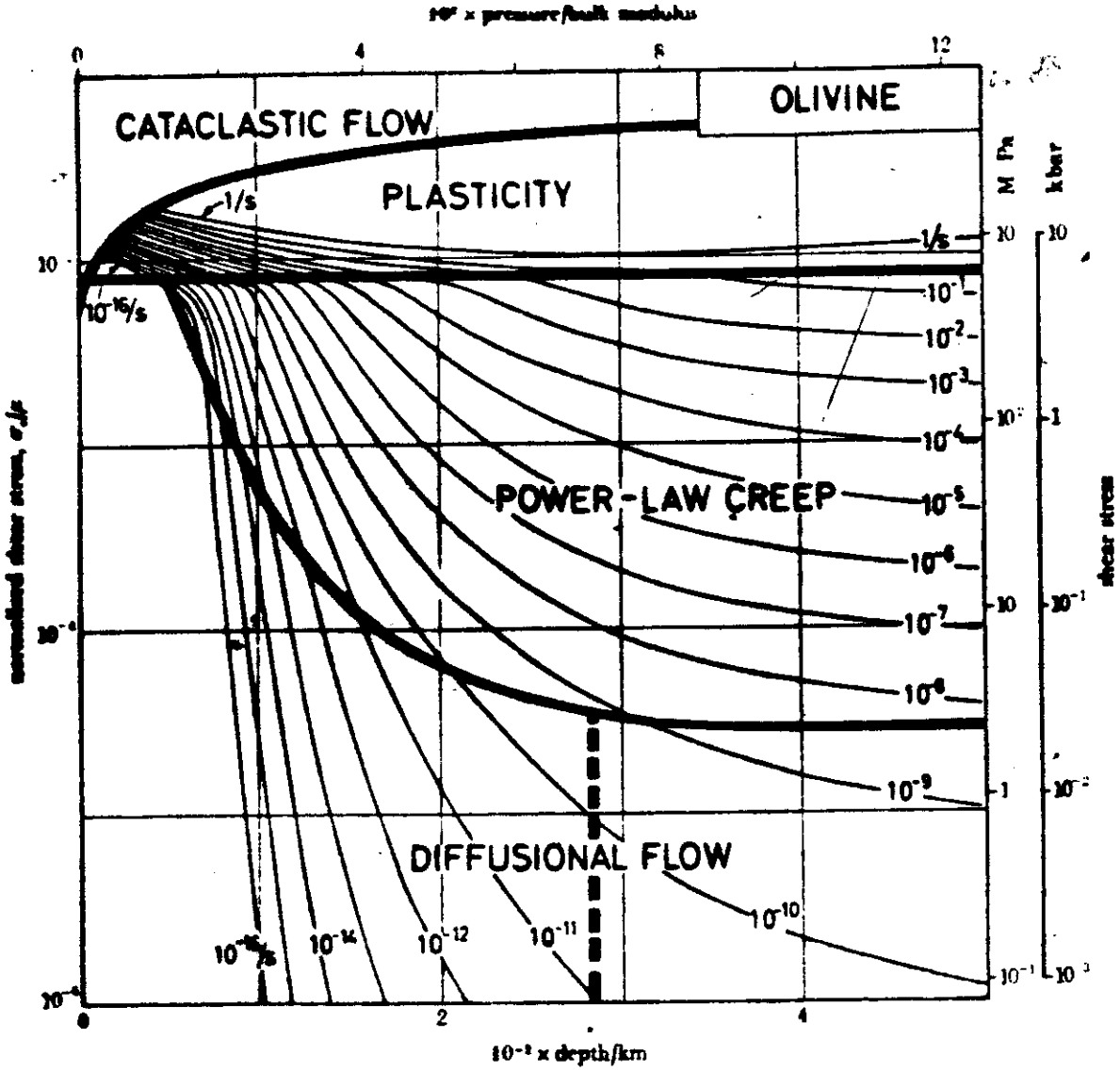

FIGURE 18. Olivine under upper-mantle conditions with $V^* = \Omega_1$. The creep rates are slower by a factor of between 10^6 and 10^8 than those of figure 17. Note that the strain-rate contours are almost flat below 200 km.

$V^* = \Omega$

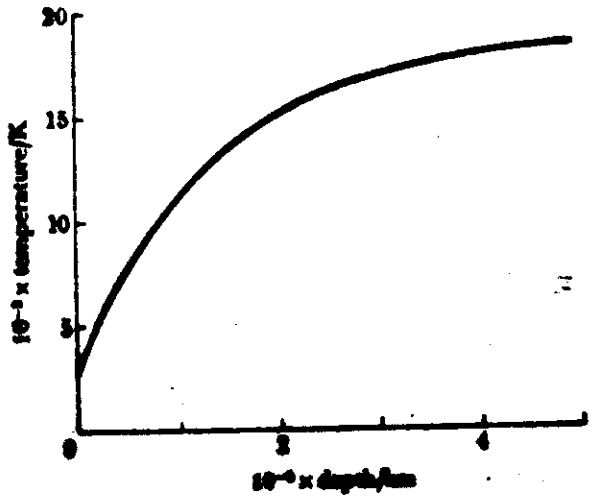

FIGURE 19. The assumed way in which temperature varies with depth in the upper mantle (see equation 8.5).

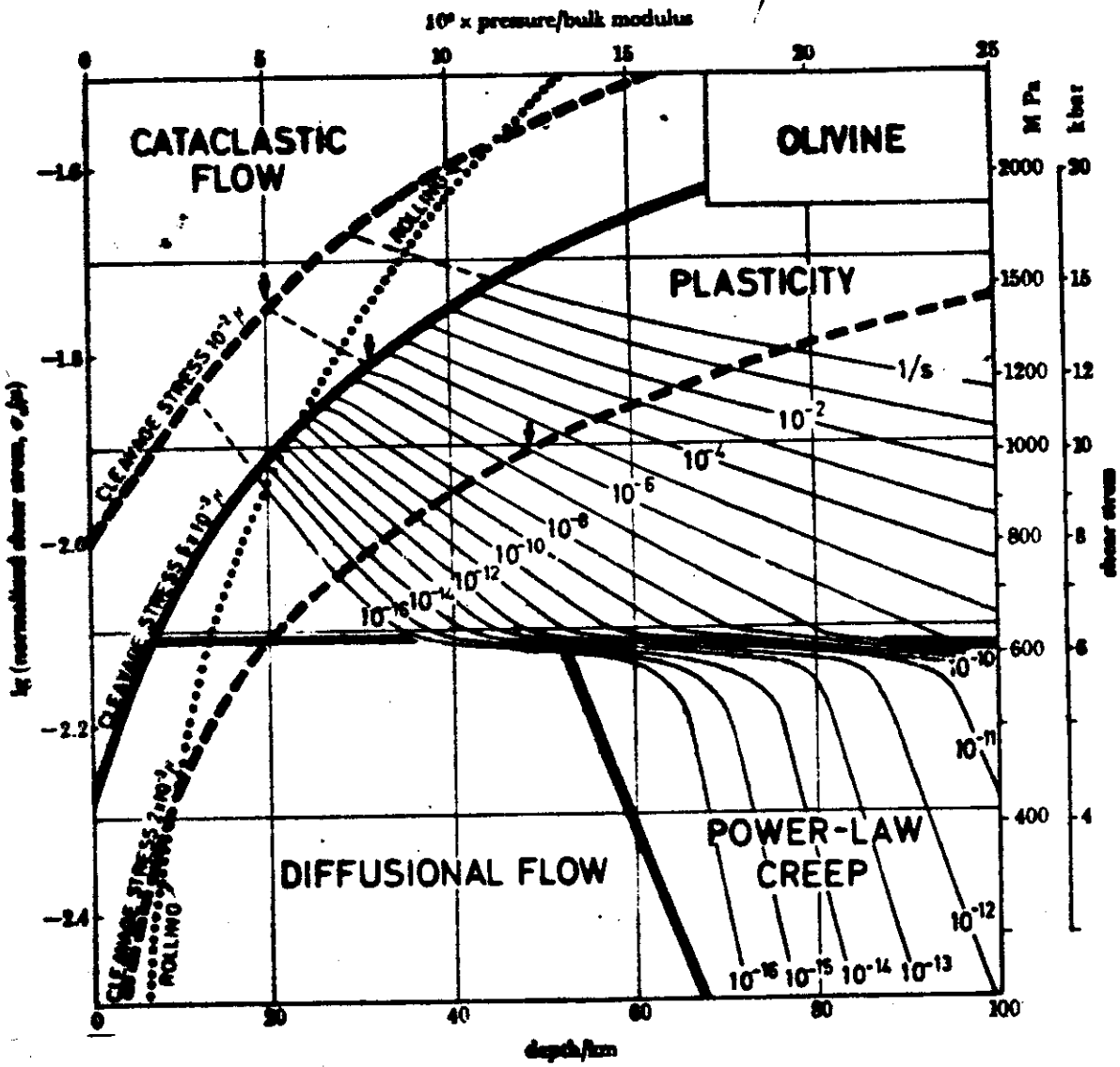

FIGURE 19. An enlarged portion of figure 18, illustrating the transition from cataclastic flow to plastic flow. The depth at which this transition occurs depends on the strain-rate and on the fracture stress, σ_f. It also depends on the temperature profile in the mantle, and will be different in regions where descending plates cool the mantle locally.

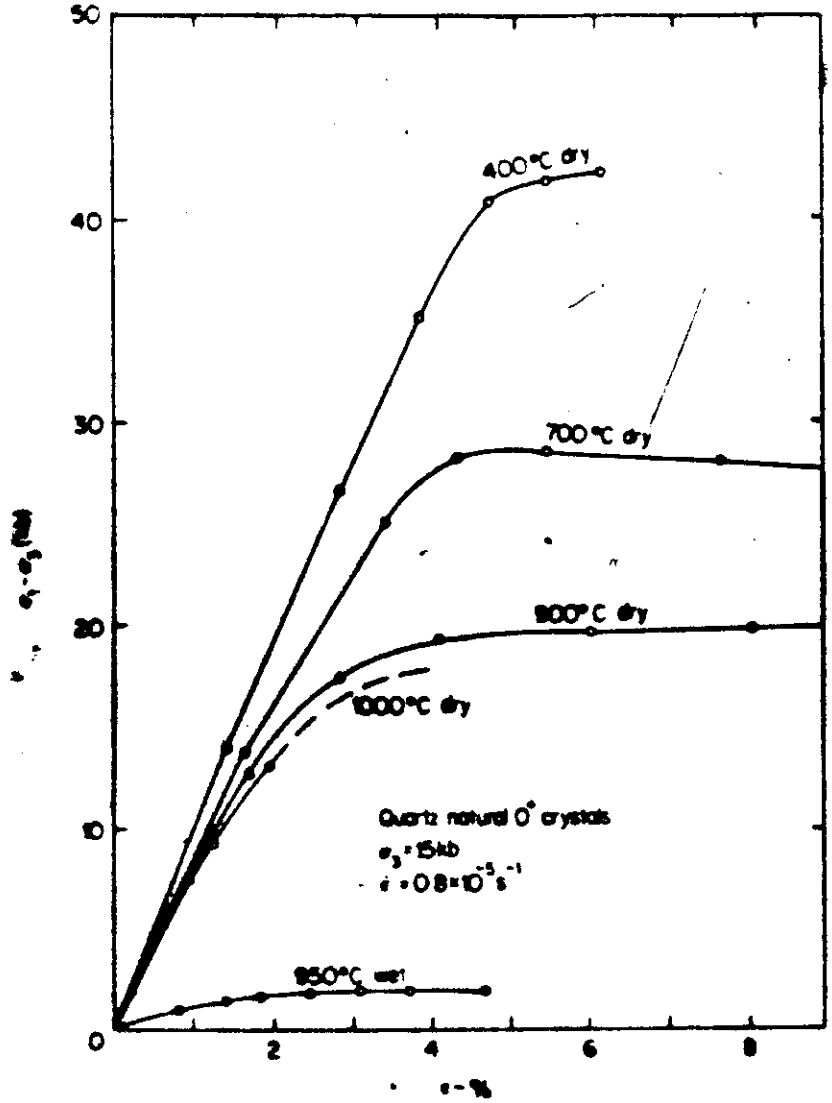

Fig. 5.30. Stress–strain curves of wet and dry natural quartz crystals (after Griggs, 1967, reproduced by permission of Blackwell Scientific Publications

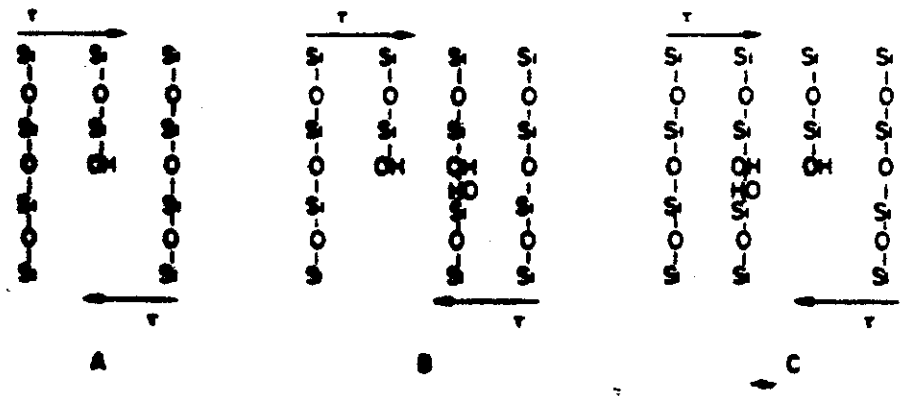

Fig. 5.31. Schematic model of the Frank–Griggs mechanism for hydrolytic weakening:
(A) Sessile hydrolysed edge dislocation with anhydrous neighbours
(B) The right-hand side neighbouring Si–O bond has been hydrolysed by arrival of a H_2O molecule and a hydrogen bond is formed
(C) The hydrogen bond can easily be broken under shear stress and reforms with the OH at the dislocation edge. As a result the dislocation moves to the right (after Griggs, 1967, reproduced by permission of Blackwell Scientific Publications Ltd.)

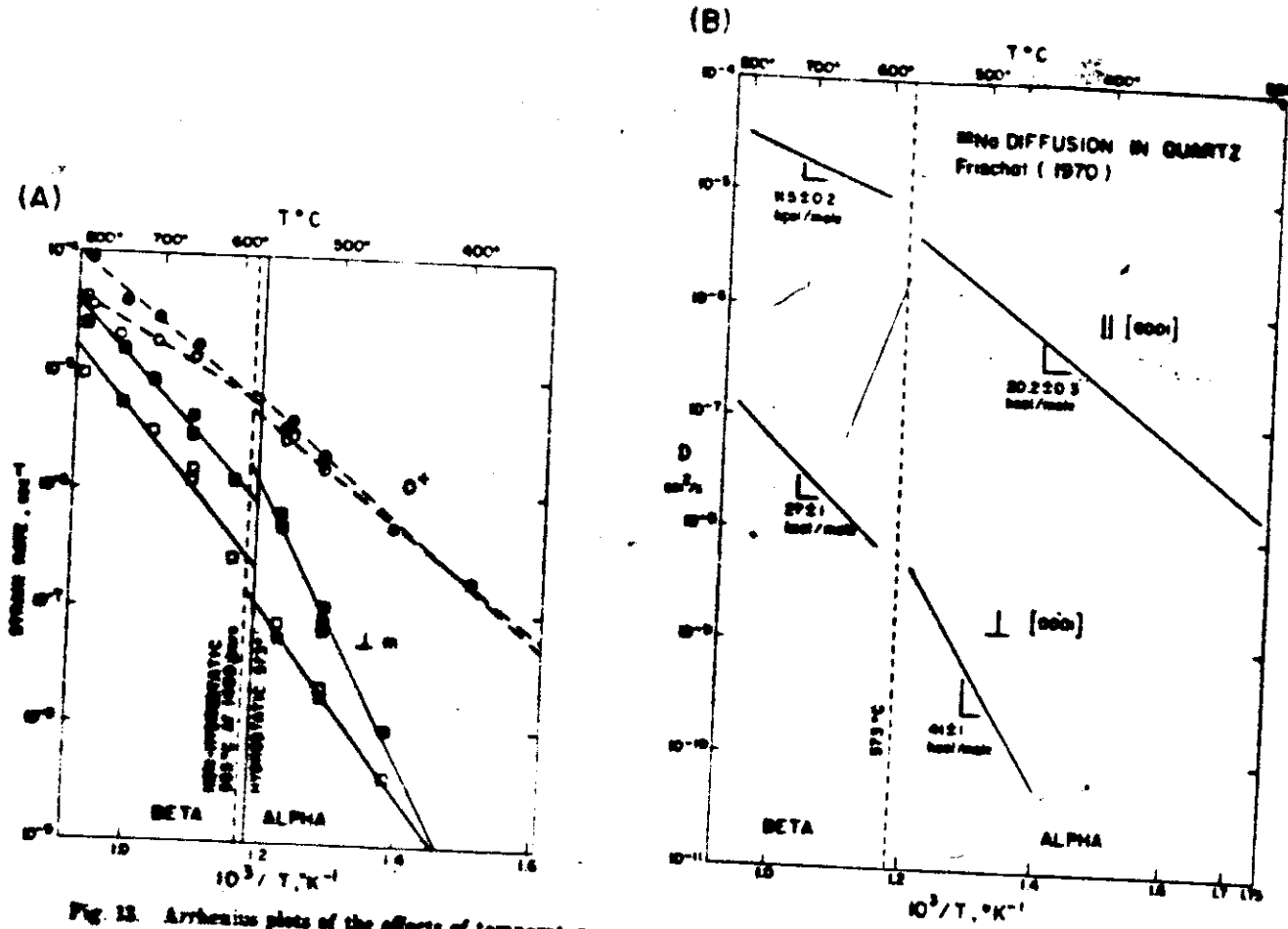

Fig. 13. Arrhenius plots of the effects of temperature on creep rates and impurity diffusion. Slopes of the data are proportional to the activation energies of the processes. (a) Creep rate variation with temperature. (b) Sodium diffusion variation with temperature. Note the remarkable way that this diffusion data mimics the creep data of (a).

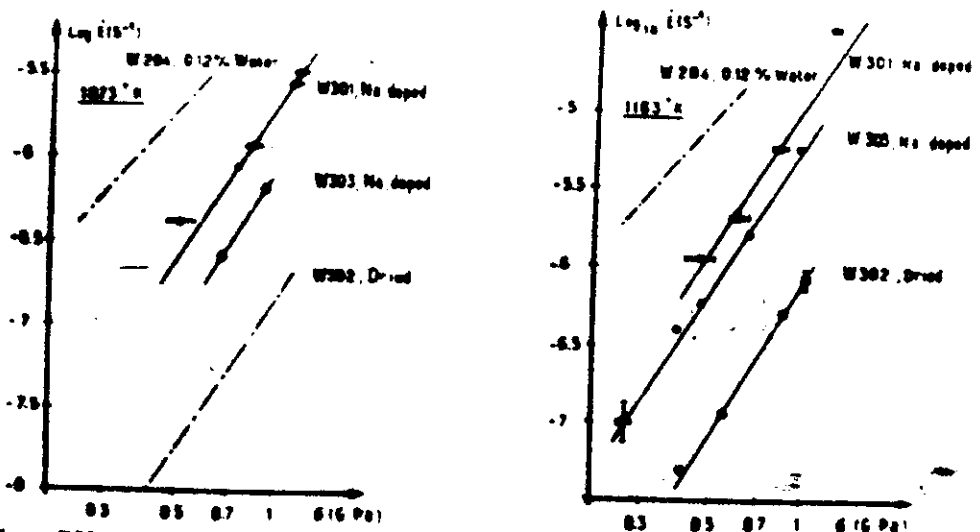

Fig. 1. Effect of impurities on the creep of quartzite at 1.5 GPa confining pressure. Total deformation of each sample is about 20%. (a) 1073°K, the investigated range is stress is somewhat narrow and high because these runs were performed mainly to make comparisons with the 1163°K data, in order to estimate the activation energies. W:302 data (dried at 1283°K under vacuum 5.5 hours) extrapolated from 1163°K to 1073°K using E = 190 kJ mol^{-1}. (b) 1163°K, the two sodium-doped samples and the "very dry" sample W:302 are compared. Note that W:284 (sample containing 0.12% by weight of water, i. e. 8700 ppm H/Si atoms) is from Jaoul et al. [this issue].

POINT DEFECT CHEMISTRY OF MINERALS AND SOLID STATE FLOW

1. Diffusion properties influenced by point defect concentrations

2. Diffusion properties control many creep mechanisms.

3. Point defect concentrations related to fugacities of volatiles.

4. In nature, once P and T fixed by overall metamorphic environment - then bulk rock chemistry buffers the fugacity of oxygen, which in turn controls the fugacity of H_2O and H_2.

For a wide range of crustal f_{O_2}, f_{H_2O} is fairly insensitive to f_{O_2} variations. $f_{H_2O} \simeq$ order of mag

f_{O_2} can be varied by several orders of magnitude by changes in bulk rock chemistry.

even from strata to strata in rock mass.

DEFECT CHEMISTRY AND CREEP

KRÖGER - VINK NOTATION

e.g. (1)

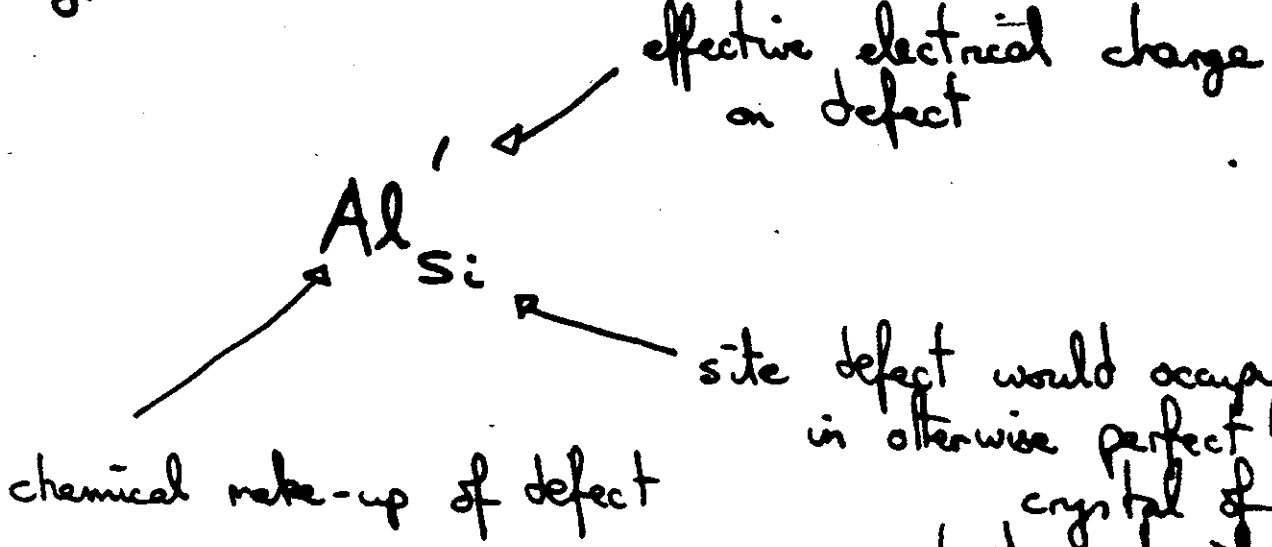

Thus in SiO_2 the above defect is -ve charged and occupies a silicon site

* = neutral defect
• = +ve defect
′ = −ve defect

eg. (2) $Si_i^{\bullet\bullet\bullet\bullet}$ = interstitial silicon with effective 4+ charge

$(OH)_i^{*}$ = interstitial neutral (OH) group.

* may be deleted.

POINT DEFECT CHEMISTRY

1. From standpoint of "hydrolytic" weakening we are interested in incorporation of hydrogen and (OH) into mineral structures.
   The mode of incorporation exerts a fundamental influence on its effects.

2. General conclusion is that hydrogen is incorporated interstitially in silicates where it acts as an electron donor.

$$H_2 \rightleftharpoons 2H_i$$

$$H_i \rightleftharpoons H_i^{\cdot} + e' \quad \leftarrow \text{conduction electron}$$

from which

$$[H_i^{\cdot}] = K_H \cdot [H_i]\, n^{-1} \quad \leftarrow \text{conc. of electrons}$$

$$= K_H^{1/2} K_H \cdot f_{H_2}^{\frac{1}{2}} n^{-1}$$

K's are equilibrium constants

3. Hydrogen can also be incorporated in other ways

eg. suggestion of Griggs that incorporation is via (HOH) group

ie $Si-O-Si + H_2O \rightleftharpoons Si-OH \cdots HO-Si$

hydrogen bond

But unless $P \sim 1$ GPa, $T \sim 900 - 1000$°C this defect has only low solubility in α-Si_3N_4. Diffusion

Point Defect Chemistry

Hydrogen incorporation (continued)

4. $(3H)_{Si}$ defect also identified { quartz + olivine

Similar defect known in hydrogarnets where $(SiO_4)^{4-}$ replaced by $(H_4O_4)^{4-}$

also $(4H)_{Si}$ defect

These are very attractive as they are embryonic water bubbles and can give infra red absorption bands when clustered.

Also can act like classical Griggs defect and diffuse with or to dislocations + facilitate their motion by introducing hydrogen bonds to be broken at dislocation cores, rather than Si-O-Si bonds.

NEUTRALITY RANGES

1. A large number of different situations are possible in silicates where the concentration of one type of defect is balanced by another so that approximate electrical neutrality is maintained.

2. However, not all of these neutrality ranges need be physically accessible since their activities may be too high or low to be meaningful or attainable.
The stability field of the mineral may also be exceeded before the required conditions are met.

3. Electrical conductivity measurements Help Here.
Charge carriers in quartz normally Na_i^+ Li^+, etc.
They are usually present in quantities to balance Al' substituted for Si sites.
Charge neutrality condition for quartz over common range of conditions is

$$[Na_i^{\cdot}] = [Al_{Si}']$$

4. Assume that in a hydrothermal environment effect is to introduce $H_i^{\cdot}$ defects (reducing environment) and $3H_{Si}'$ defects (oxidizing environment).

Thus as f_{H_2O} or f_{H_2} increases around quartz

$[Na_i^{\cdot}] = [(3H)_{Si}']$ oxidizing

$[Al_{Si}^{\cdot}] = [H_i^{\cdot}]$ reducing

At very high f_{H_2O}

$[H_i^{\cdot}] = [(3H)_{Si}']$

DEFECT CHEMISTRY AND CREEP

Pure Quartz

① $-Si \rightleftharpoons Si_{si} + 2V_o$ silicon incorporation

② $O_2 \rightleftharpoons 2O_o + V_{Si}$ oxygen incorporation

③ $V_o \rightleftharpoons V_o^{\cdot\cdot} + 2e'$ } formation of vacancies

④ $V_{Si} \rightleftharpoons V_{Si}^{''''} + 4h^{\cdot}$ }

Law of Mass Action gives

eg. ① $[Si_{si}][V_o]^2 = K_{Si} a_{Si}$

K_{Si} = equilibrium constant for reaction ①

② $[O_o]^2[V_{Si}] = K_o a_{O_2}$

K_o is equilibrium constant for reaction ②.

Establish reaction, and law of mass action gives concentration of defects as f(volatile)

Impose electro neutrality condition that overall charge of xstal should be neutral

Then equations for concentration of certain key defects can be simplified.